DOI: 10.1002/anie.200805257

Chromophores and π Systems

Two-Photon Absorption and the Design of Two-Photon Dyes

Miłosz Pawlicki, Hazel A. Collins, Robert G. Denning, and Harry L. Anderson**

Keywords:
chromophores · photodynamic therapy · porphyrinoids · two-photon absorption · uncaging

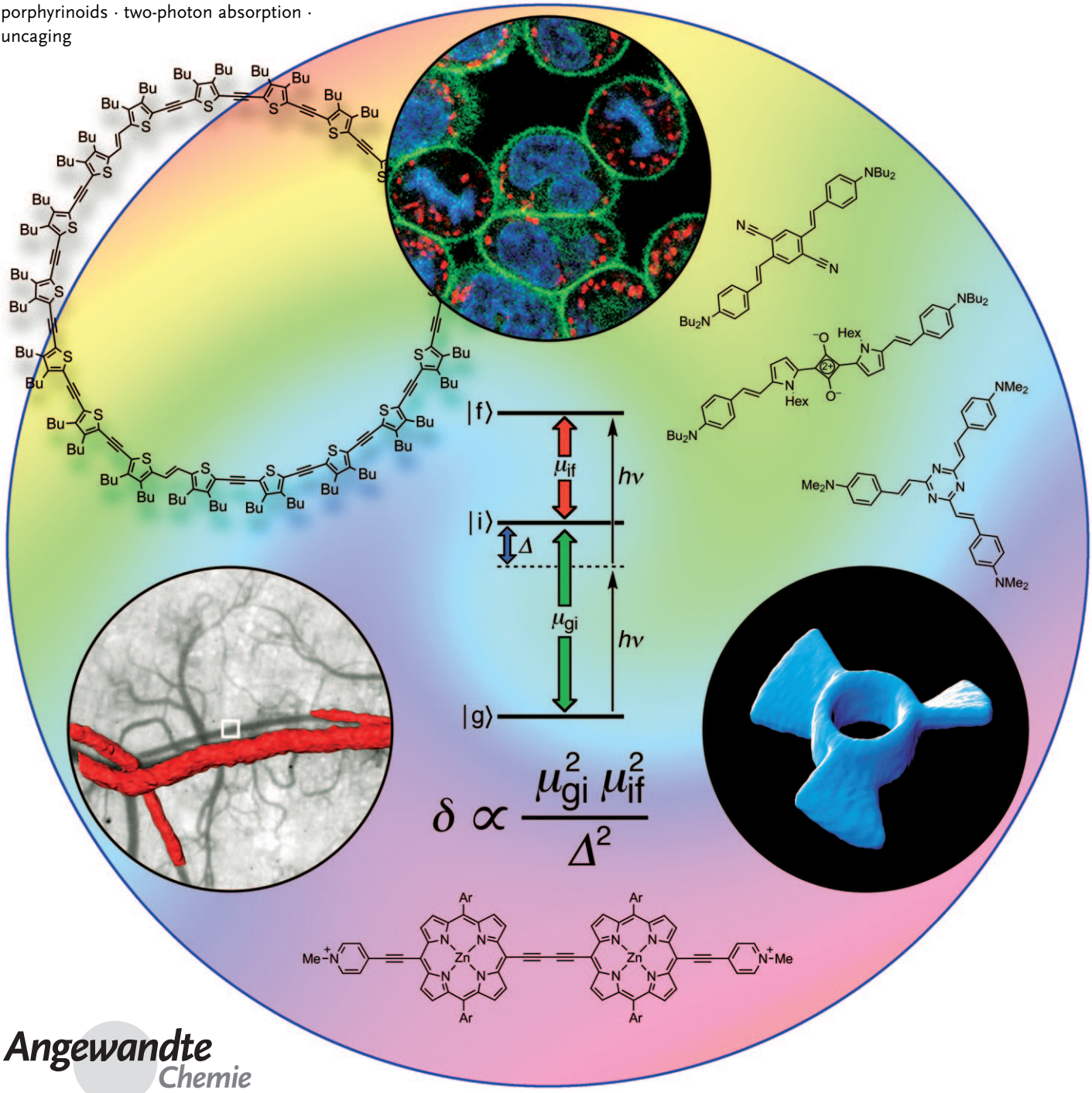

Angewandte Chemie

Two-photon absorption has important advantages over conventional one-photon absorption, which has led to applications in microscopy, microfabrication, three-dimensional data storage, optical power limiting, up-converted lasing, photodynamic therapy, and for the localized release of bio-active species. These applications have generated a demand for new dyes with high two-photon absorption cross-sections. This Review introduces the theory of two-photon absorption, surveys the wide range of potential applications, and highlights emerging structure–property correlations that can serve as guidelines for the development of efficient two-photon dyes.

From the Contents

1. Introduction

The simultaneous absorption of two photons by the same molecule was first analyzed theoretically in the 1930s by Göppert-Mayer (Figure 1),[1] and was first demonstrated experimentally in 1961,[2] soon after the invention of the laser. Two-photon absorption became easier to investigate as sub-picosecond pulsed lasers became more readily available in the 1990s (particularly the Ti:sapphire laser). The invention of two-photon fluorescence microscopy by Webb and co-workers,[3] and the rapid adoption of this technique by manufacturers of confocal microscopes, has led to an explosion of interest in all types of multiphoton processes.[4]

Figure 1. Maria Göppert-Mayer developed the theory of two-photon absorption (2PA) in the 1930s, at about the time that she completed her PhD. The GM unit of 2PA cross-section is named after her. She was awarded the Nobel Prize in Physics in 1963 for theoretical work on the structures of atomic nuclei.

The main difference between one-photon absorption (1PA) and two-photon absorption (2PA) is that 2PA involves the simultaneous interaction of two photons, and so it increases with the square of the light intensity, whereas 1PA depends linearly on the intensity. This is the reason why 2PA is only observed in intense laser beams, particularly focused pulsed lasers, which generate a very high instantaneous photon density. Most of the applications for 2PA result from this intensity dependence. 2PA is a way of accessing a given excited state by using photons of half the energy (or twice the wavelength) of the corresponding one-photon transition, thus leading to other applications. In this Review we only consider simultaneous 2PA, not processes involving the stepwise absorption of two photons (which we call excited-state absorption, ESA). We also only consider degenerate 2PA, in which both photons have the same energy.

There is now a strong demand for efficient 2PA dyes for a wide range of applications, including microscopy,[5,6] microfabrication,[7] three-dimensional data-storage,[8,9] optical power limiting,[10] up-converted lasing,[11] photodynamic therapy,[12] and for the localized release of bio-active species.[13] Recently, this demand has been matched by rapid advances in the design and synthesis of 2PA dyes. This field has been comprehensively reviewed.[14] Here we identify the key principles and emerging structure–property relationships, and illustrate these concepts by comparing the behavior of a small number of selected chromophores. We conclude by discussing the design of two-photon dyes for the most prominent applications.

[*] Dr. M. Pawlicki, Dr. H. A. Collins, Prof. R. G. Denning, Prof. H. L. Anderson
Department of Chemistry, University of Oxford
Chemistry Research Laboratory
12 Mansfield Road, Oxford, OX1 3TA (UK)
Fax: (+44) 1865-285-002
E-mail: bob.denning@chem.ox.ac.uk
harry.anderson@chem.ox.ac.uk
Homepage: http://hla.chem.ox.ac.uk/

2. Theory of Two-Photon Absorption

2.1. Fundamental Principles

Using assumptions equivalent to those of the Beer–Lambert law for 1PA, the attenuation of a beam of light resulting solely from 2PA, is given by Equation (1):

$$\partial I/\partial z = -N\,\alpha_2\,I^2 = -N\,\delta\,F\,I \tag{1}$$

where I is the intensity, z is the distance into the medium, N is the number of molecules per unit volume, and α_2 is a molecular coefficient for 2PA. The intensity can also be expressed as a photon flux $F = I/h\nu$ (with units of photons $s^{-1}cm^{-2}$; $h\nu$ is the photon energy), in which case the coefficient δ in Equation (1) is adopted and is usually reported in Göppert-Mayer units ($1\,GM \equiv 10^{-50}\,cm^4\,s\,photons^{-1}\,molecule^{-1}$). δ is known as the molecular 2PA cross-section.

If the light is plane-polarized, the value of δ for a transition from the ground state g to a final state f at the maximum of a 2PA band with a Lorentzian line shape is given by Equation (2).[15–18]

$$\delta_{max} = \frac{2\pi h\nu^2\,L^4}{\varepsilon_0^2\,n^2\,c^2}\left(\frac{1}{\Gamma}\right)S_{fg} \qquad \text{where } S_{fg} = \left[\sum_i \frac{\langle \boldsymbol{\mu}_{gi}\,\boldsymbol{\mu}_{if}\rangle}{(E_{gi}-h\nu)}\right]^2 \tag{2}$$

Here, E_{gi} is the energy gap between the ground state and an intermediate state i, and Γ is the half-width at half-maximum of the 2PA band in energy units. The summation is over all the states of the molecule. The factor $L = (n^2+2)/3$ (where n is the refractive index) represents the enhancement of the optical field in the medium relative to that in a vacuum. The term $\boldsymbol{\mu}_{kl}$ is the amplitude of the oscillating (transition) dipole moment (or polarization) induced by the electric field of a light wave whose frequency matches (is in resonance with) the energy difference between the k and l states. The various transition dipole moment vectors $\boldsymbol{\mu}_{kl}$ rotate with the molecule in solution, so an average must be made of their projection onto the direction of the optical field, over all orientations of the molecule—this is the meaning of the pointed brackets in Equation (2). This average is not straightforward,[19] but the result is 1/5 if all the moments $\boldsymbol{\mu}_{gi}$ and $\boldsymbol{\mu}_{if}$ are co-parallel. This is true of the great majority of strong two-photon absorbers, so we may omit the vector notation to give, after some rearrangement, Equation (3):

$$S_{fg} = \frac{1}{5}\left[\underbrace{\left(\frac{\Delta\mu_{gf}\,\mu_{gf}}{h\nu}\right)^2}_{\text{D term}} + \underbrace{\sum_{i\neq f,g}\left(\frac{\mu_{gi}^2\,\mu_{if}^2}{(E_{gi}-h\nu)^2}\right)}_{\text{T term}}\right] \tag{3}$$

where $\Delta\mu_{gf}$ is the change in the static dipole moment in the final state relative to the ground state. The two parts of Equation (3) have been described as the "dipolar" D term and "two-photon" T term, respectively.[20]

2.2. Essential State Models

All static dipole moments are zero and the D term is absent in centrosymmetric molecules. The 2PA cross-section is often dominated by the interaction of the ground state with just two excited states. In such cases the sum in Equation (3) is reduced to a single term, and the 2PA cross-section can be approximated by Equation (4), where C is a constant.

$$\delta_{max} \approx C\,\frac{\mu_{gi}^2\,\mu_{if}^2}{((E_{gi}/h\nu)-1)^2\,\Gamma} \tag{4}$$

The three "essential" states in this model have alternating symmetry: both the ground-state and the final-state wavefunctions, $|g\rangle$ and $|f\rangle$, respectively, are *gerade* (that is, symmetric with respect to the center of inversion), whereas

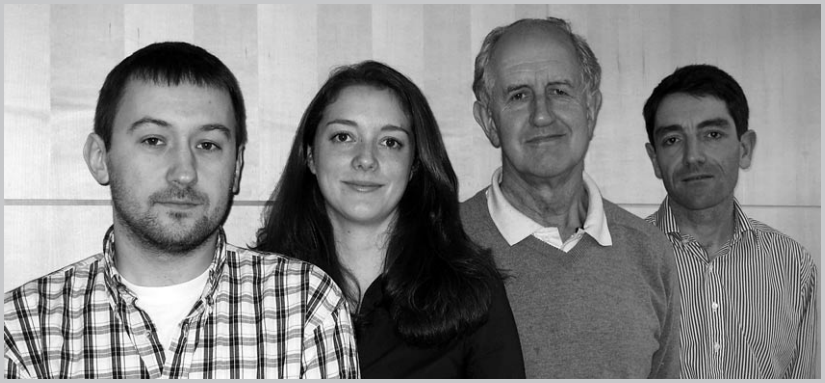

Miłosz Pawlicki (left) completed his PhD at the University of Wrocław, Poland in 2004 under the mentorship of Lechosław Latos-Grażyński. He is currently a Marie Curie Research Fellow, working on the synthesis of porphyrin-based two-photon dyes in Oxford.
Hazel A. Collins (second left) completed her PhD with Harry Anderson at Oxford University in 2008 on two-photon-excited photodynamic therapy, and is currently exploring dyes for nonlinear optical imaging of biological structures.
Robert G. Denning (second right) is an Emeritus Professor of Chemistry at Oxford University. His work is centered round the optical properties of condensed matter, and makes use of laser spectroscopy as well as measurements of nonlinear optical parameters.
Harry L. Anderson (right) completed his PhD at Cambridge University (UK). After postdoctoral work at ETH Zürich (Switzerland), he was appointed to a lectureship in Oxford in 1994. His research concerns the design and synthesis of molecular and supramolecular optoelectronic materials, with particular emphasis on conjugated porphyrin oligomers and cyclodextrin-encapsulated π systems.

the intermediate state $|i\rangle$ is *ungerade* (that is, antisymmetric). For a linear molecule of D_{2h} symmetry, these states are labeled $1A_g$, $1B_{1u}$, and $2A_g$ as shown in Figure 2a.[21,22]

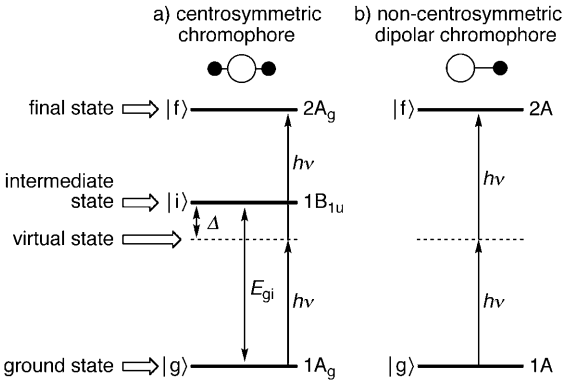

Figure 2. Energy level diagrams for the essential states in a) centrosymmetric and b) non-centrosymmetric chromophores. The states are labeled for D_{2h} and C_2 symmetry, respectively, but the diagram is general to the lowest 2PA transition in any centrosymmetric or non-centrosymmetric molecule.

Transitions are one-photon electric-dipole-allowed for both $g \leftrightarrow i$ and $i \leftrightarrow f$. In the case of 2PA, the optical frequency ν is out of resonance with both these transitions, but it creates a nonstationary (namely, virtual) state that is a superposition (or mixture) of $|g\rangle$ and $|i\rangle$, in which the induced polarization is detuned from that in the intermediate state by a frequency difference that corresponds to an energy $\Delta = E_{gi} - h\nu$. This "virtual state" only exists while the molecule experiences the field of the first photon (about 5 fs).[23] The transient presence of $|i\rangle$ with *ungerade* parity in this superposition allows the second photon at frequency ν to induce an electric-dipole transition to the final *gerade* state $|f\rangle$. The $1A_g \leftrightarrow 2A_g$ transition is, therefore, allowed in 2PA, but forbidden in 1PA. This reversal in selection rules between 1PA and 2PA is general to all centrosymmetric chromophores.

In non-centrosymmetric molecules, the $g \leftrightarrow f$ transition of Figure 2b is electric-dipole allowed and the D term of Equation (3) is non-zero. In this case, $|f\rangle$ plays the role of $|i\rangle$, and the transition now appears in both 1PA and 2PA. The T term makes a smaller contribution in dipolar chromophores because it relates to higher states (now $|i\rangle$ lies above $|f\rangle$, so $\Delta > h\nu$). If $|i\rangle$ lies below $|f\rangle$ (as in Figure 2a), then $\Delta < h\nu$ and (assuming $\Delta\mu_{kl} \approx \mu_{kl}$) the D term for dipolar chromophores in Equation (3) is intrinsically smaller than the T term for centrosymmetric systems. This explains in part why most dipolar 2PA chromophores have smaller cross-sections than comparable quadrupolar analogues.

The magnitudes of μ_{gi}^2 and μ_{gf}^2 are proportional to the one-photon oscillator strengths, so their values can be calculated from the linear absorption spectrum. However, μ_{if} is rarely determined experimentally, so the design of efficient 2PA chromophores has proceeded empirically, with guidance from theoretical calculations of transition moments. Adding an electron donor D and acceptor A to the ends of a conjugated chromophore to give a D-π-A system enhances μ_{gf}^2 as a consequence of the increase in the displacement of charge during the transition from a donor-centered HOMO to an acceptor-centered LUMO. Centrosymmetric analogues with D-π-A-π-D or A-π-D-π-A structures exploit the same principle and are efficient 2PA chromophores.[24,25]

2.3. Molecular Orbital Descriptions

Accurate calculations of δ need to include electron-correlation effects known as configuration interaction (CI),[21] and thus the excited states cannot be depicted by simple changes in the occupancy of elementary molecular orbitals. Fortunately, this difficulty can be significantly alleviated by using "natural transition orbitals",[26] which enable the role of the various singly excited configurations that contribute to an excited state to be visualized in the form of "electron" and "hole" distributions. As an example, Figure 3 shows the

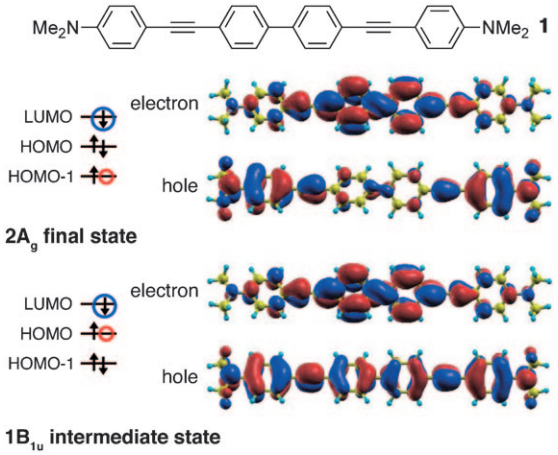

Figure 3. Electronic structure of the $2A_g$ and $1B_{1u}$ excited states of **1**. The occupancies of the LUMO, HOMO, and HOMO-1 energy levels are illustrated on the left, and natural transition orbitals for the "electron" and "hole" in each state are shown on the right.[27]

charge displacements, obtained by a time-dependent DFT calculation, associated with μ_{gi} and μ_{if} in compound **1**, which has a 2PA band at about 700 nm with $\delta_{max} \approx 500$ GM that corresponds to the $1A_g \rightarrow 2A_g$ transition at 3.54 eV, and a 1PA band corresponding to the $1A_g \rightarrow 1B_{1u}$ transition at 3.31 eV.[27] In the intermediate $1B_{1u}$ state, the hole is uniformly spread along the length of the chromophore, whereas the electron is localized around the center of the molecule. Thus, the $1A_g \rightarrow 1B_{1u}$ transition results in a net displacement of charge from the electron-rich terminals towards the biphenyl core. The distribution of the electron in the final $2A_g$ state is almost identical to that in the $1B_{1u}$ intermediate state, but the hole now becomes localized on the terminals, further increasing the quadrupolar polarization.

Figure 4 gives a grossly simplified representation of this process, ignoring the effects of CI (in which every node in the transition orbitals of Figure 3, other than that normal to z at the center of inversion, has been removed). The polarization μ_{gi} driven by the optical field of the first photon (Figure 4a) is represented by the superposition (mixing) of the HOMO and

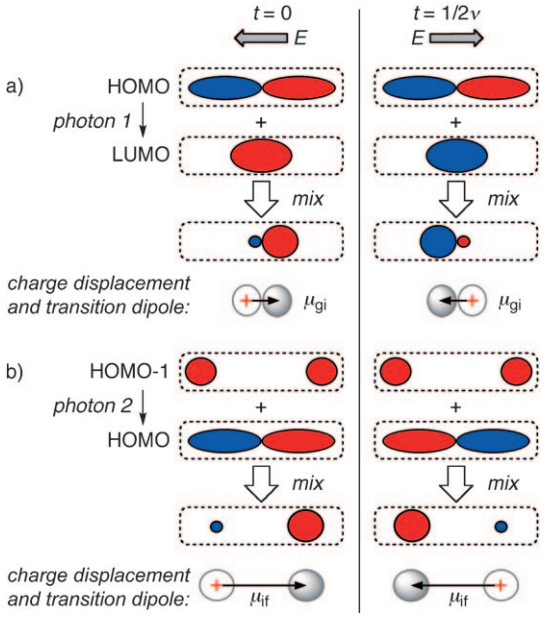

Figure 4. Simplified representation of wavefunctions and transition dipole moments for $|g\rangle \rightarrow |i\rangle$ (a) and $|i\rangle \rightarrow |f\rangle$ transitions (b) in **1**. Off-resonance ($h\nu \neq E_{gi}$) for the process in (a) gives a transient virtual state. The two columns show two instants in the optical field cycle separated by a time interval of $1/2\nu$ (π phase shift), during which the optical electric field E changes direction. Red and blue represent positive and negative amplitudes of the wavefunctions, respectively.

LUMO wavefunctions, whose intrinsic (standing-wave) frequencies differ by the resonant transition frequency ν. The HOMO–LUMO mixing is represented by the addition of their amplitudes to give a hybrid, in which the amplitude is large on one side of the center but small on the other side. This result implies that there is a momentary dipolar displacement of charge. At two points in the optical cycle (see Figure 4) with a phase-separation of π at the resonant frequency, the mixing results in opposed dipolar displacements of charge with magnitude μ_{gi}. Notice that μ_{gi} should be integrated over a complete optical cycle, in each half of which charge is drawn towards the center from opposite ends of the D-π-A-π-D unit. An analogous single-ended D-π-A chromophore would only be polarizable in one direction (D→A), so it would only be influenced by half of the polarization cycle, thus reducing the magnitude of μ_{gi}.

When the optical field is on resonance, as it is in an allowed 1PA transition, it remains in-phase with the polarization and establishes a finite transition probability. When it is off-resonance, as in the 2PA case, the phases match only transiently—there is no 1PA transition probability, and the polarization at the optical frequency is damped and small. Nevertheless, the incipient presence of a hole in the HOMO and an electron in the LUMO provides a foothold for a second photon to drive the HOMO-1→HOMO transition (Figure 4b). The final outcome of 2PA is a hole in HOMO-1 and an electron in the LUMO, and this causes a quadrupolar displacement of charge from the ends to the center that can be described by the function $(2z^2-x^2-y^2)$—which has the form of the angular part of a d_{z^2} orbital.

2.4. Evolution of δ with Chromophore Length

The 2PA cross-section of a molecule depends strongly on the length of its conjugated π system, and thus on the number of π electrons N_e. Since the transition moments μ_{kl} are related to the distance over which the charge is displaced during a transition, they might be expected to scale with the length of a linear chromophore, thus giving $\mu \propto N_e$. However, as the π system becomes longer it reaches a length, known as the "conjugation length", beyond which—because of factors such as loss of conformational planarity—the coherence of the wavefunction is not maintained and the electrons become confined to segments of the chain. At this point, μ reaches a maximum value that is independent of the notional length of the conjugated chain. Thus, the conjugation length is a measure of the extent of π delocalization. It is difficult to predict the dependence of δ on the length of a π system, since there are no simple expressions for the dependence of E_{gi}, $h\nu$, or Γ in Equation (4) on N_e. However these parameters can be measured experimentally, so a new quantity, called the conjugation signature S_C, can be defined by Equation (5).[28]

$$S_C = \delta_{max}\,\Gamma((E_{gi}/h\nu)-1)^2 = C\mu_{gi}^2\mu_{if}^2 \quad (5)$$

Since S_C depends only on the product of the transition dipole moments, it should be a good indicator of the effective conjugation length. One expects that $S_C \propto N_e^4$ for fully conjugated systems, and that $S_C \propto N_e$ for a molecule consisting of a set of small uncoupled chromophoric units. The value of the exponent k in the scaling law $S_C \propto N_e^k$ provides insight into the strength of the π conjugation. As N_e increases in a series of linear oligomeric chromophores, k shifts from 4 to 1 as δ reaches saturation (see Section 4.1.2.3 for examples and further discussion of this concept).

2.5. Conclusions from Theory

The requirements for maximizing the 2PA cross-section of a chromophore include:

1) Long, π-conjugated chains with enforced coplanarity that ensure large conjugation lengths that lead to high values of μ_{gi}, μ_{if}, μ_{gf}, and/or $\Delta\mu_{gf}$ [Eq. (3)].
2) Donor and acceptor groups at the center and ends of the molecule that can also enhance μ_{gi}, μ_{if}, μ_{gf}, and/or $\Delta\mu_{gf}$.
3) Centrosymmetric chromophores that possess a strong 1PA transition close to the 2PA laser wavelength, thus enhancing the δ value when the Δ value is small [$\Delta = E_{gi} - h\nu$; Figure 2a and Equation (3); if $\Delta = 0$, then 2PA will be difficult to observe because of overlap with the 1PA].
4) Chromophores with narrow one- and two-photon absorption bands. Since the area of a 2PA band is fixed by the value of S_{fg}, a narrow 2PA band (with small Γ) leads directly to a high δ_{max} value [Eq. (2)]. In centrosymmetric chromophores, the requirement for the intermediate state to be close to, but not overlapping with, the virtual state leads to a need for a sharp 1PA band.

Two factors are important when comparing the lowest energy 2PA bands of centrosymmetric and non-centrosymmetric chromophores:

a) The possibility of resonance with an intermediate state $|i\rangle$, of roughly half the energy of the final state $|f\rangle$, leads to a large T term in Equation (3) and enhances the 2PA of a centrosymmetric chromophore. In a dipolar chromophore, there can be no intermediate state that is one-photon allowed but two-photon forbidden.
b) The transition moment μ_{gi} in a D-π-A-π-D system will be larger than μ_{gf} for the corresponding D-π-A unit, since D-π-A-π-D will be effectively polarized by both parts of the optical field cycle, whereas D-π-A is easily polarized in just one direction.

Both these factors tend to make the T term in Equation (3) larger than the D term, and lead to stronger 2PA in centrosymmetric chromophores.

3. Measurement of 2PA Cross-Sections and 2PA Spectra

Before discussing the structure–property relationships that are emerging from the very wide range of chromophores that have been studied experimentally, something needs to be said about the techniques used for measuring 2PA cross-sections. δ values can be strongly influenced by the measurement technique because of a variety of artifacts.

The two main techniques for measuring 2PA cross-sections are known as *z*-scan and two-photon excited fluorescence (TPEF). Other techniques which provide less direct information on 2PA cross-sections (such as degenerate four-wave mixing) or which are less widely used (such as the white-light continuum method, fs-WLC) are beyond the scope of this Review.

3.1. The z-Scan Technique

The *z*-scan method involves moving a sample along the path of a focused laser beam and measuring the light intensity at the detector as a function of its position along this *z*-axis, as summarized in Figure 5.[29] If the detector has a narrow aperture (as in the so called "closed-aperture" setup), then the output is sensitive to intensity-dependent changes in the refractive index (as a result of third-order nonlinear polarizability or thermal effects) which lead to self-focusing or defocusing of the beam. Alternatively, if the detector collects all the light from the sample ("open-aperture" setup), then the output only reflects the intensity-dependent transmission,

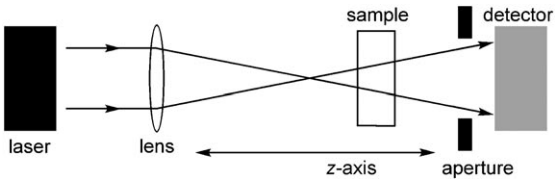

Figure 5. Experimental setup for the *z*-scan experiment.

and can be used to measure 2PA cross-sections. Two effects other than true simultaneous two-photon absorption can contribute to the apparent 2PA cross-sections measured by open-aperture *z*-scan experiments:[29,30]

1. Light can be lost due to self-defocusing (if the aperture of the detector is too narrow or too far from the sample) or because of nonlinear scattering; this results in extra contributions to the apparent nonlinear absorption.
2. A build up of excited-state populations (by either one-photon or two-photon absorption) can lead to nonlinear transmission through excited-state absorption (ESA). The contribution from ESA can be reduced by the use of wavelengths where there is negligible 1PA, very short laser pulses (<1 ps), and low repetition rates; a repetition rate of less than 1 kHz may be needed to allow excited triplet states to fully decay between pulses.

The *z*-scan technique is very useful for probing nonlinear transmission (for example, in the context of optical power limiting; Section 5.9) and for characterizing nonlinear refraction (using a closed aperture). However, the two problems mentioned above can be difficult to avoid, and tend to enhance the apparent 2PA cross-section. For example, it has been shown that thermal lens effects can lead to substantial artifacts in 2PA cross-sections measured by the *z*-scan technique, even when using femtosecond pulses, a 1 kHz repetition rate, and a wavelength at which there is negligible one-photon absorption.[30]

3.2. Two-Photon Excited Fluorescence (TPEF)

The TPEF intensity provides direct information on the efficiency of 2PA. Several variants of this experiment have been developed since it was first reported by Xu and Webb.[31] If a suitable reference compound with a known 2PA spectrum is available, then the simplest approach is to compare the one- and two-photon excited fluorescence excitation spectra of the sample and this reference sample under identical conditions. This double-referencing method enables a large number of variables to be automatically cancelled. Thus, it is not necessary to know parameters relating to the excitation light (pulse energy, pulse duration, and temporal intensity distribution), the wavelength dependence of the efficiency of the detector, nor the concentration and fluorescence quantum yield of the sample. However, any uncertainty in the one-photon extinction coefficient ε leads directly to uncertainty in the value of δ. The TPEF technique has been optimized extensively by Rebane, Drobizhev, and co-workers,[32] and they recently reported accurate reference 2PA spectra for a wide range of commercially available dyes, thus making the TPEF method particularly attractive.[33]

TPEF experiments require the use of a pulsed laser, typically about 100 fs, although in contrast to the *z*-scan method, the accuracy of δ values from TPEF is not strongly dependent on the pulse width.[25] As with most fluorescence measurements, a dilute solution is used (with an optical density of about 0.1), so small amounts of material are required. The intensity of the TPEF signal increases with the

square of the laser intensity; it is important to check this quadratic power dependence, to avoid overestimating the δ value because of fluorescence contributions from 1PA. Thus, two limitations of this technique are: 1) it cannot be applied in spectral regions with one-photon absorption and 2) the sample must be photoluminescent. However, the first of these restrictions is general to all techniques for measuring reliable two-photon cross-sections. The second restriction can be overcome in some cases by quantifying a secondary photochemical process, such as the luminescence from singlet oxygen generated by energy transfer from the 2PA-generated triplet excited state of the chromophore.

In practice, 2PA cross-sections from *z*-scan measurements (even using femtosecond pulses) often appear to be exaggerated when compared with TPEF values.[34] Here we focus, where possible, on values from femtosecond two-photon fluorescence (fs-TPEF).

Single-wavelength measurements of two-photon cross-sections are quick to record, but it is more informative to compare whole spectra. Here we discuss maximum values δ_{max} of the 2PA cross-sections; if these are not available we report single-wavelength δ values. The errors in the determination of the 2PA cross-sections are generally greater than 10%, even under the best experimental conditions, so in the following sections all δ values are quoted to two significant figures.

4. Design Strategies and Structure–Property Relationships

4.1. Linear Chromophores

Two-photon absorption by organic dyes was first demonstrated experimentally in 1963,[35] but it was only many years later that structure–property relationships emerged for the rational design of 2PA chromophores. In 1997, Marder, Perry, and co-workers reported a comparison of *trans*-stilbene (**2**)

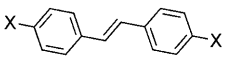

2, X = H, δ_{max} = 12 GM at 514 nm (fs-TPEF)
3, X = NBu_2, δ = 110 GM at 620 nm (fs-TPEF)
4, X = NPh_2, δ_{max} = 340 GM at 680 nm (fs-TPEF)

and its derivative **3** with terminal donor substituents.[36] The 2PA cross-section of **3** (110 GM) is almost ten times higher than that of the unsubstituted stilbene (**2**; a further increase was observed for **4** with diphenylamine substituents).[24,33] The discovery that centrosymmetric charge transfer results in high 2PA cross-sections led to a general approach for the design of 2PA chromophores, with two donor (D) or acceptor (A) terminals linked by a π-conjugated bridge.[24]

While Marder, Perry, and co-workers were exploring centrosymmetric chromophores, Reinhardt, Prasad, and co-workers developed dipolar dyes with polarizable bridges.[37] These D-π-A dyes exhibited strong apparent two-photon absorption from nanosecond *z*-scan measurements, but subsequent femtosecond measurements gave significantly lower values in most cases (< 100 GM).[38] A few dipolar systems with rather high 2PA cross-sections, such as **5**[39] and **6**,[33] have been reported recently, but dipolar systems, in general, seem to give weaker 2PA than centrosymmetric dyes of the same size and complexity.

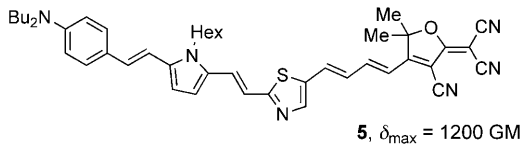

5, δ_{max} = 1200 GM at 1440 nm (fs-WLC)

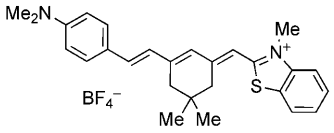

6, δ_{max} = 730 GM at 1250 nm (fs-TPEF)

Variation of the donor and acceptor substituents has now become a popular approach to creating new two-photon dyes. The research groups of Marder,[24,39–41] Prasad,[37,42,43] and Blanchard-Desce[27,44–48] are the leading pioneers in this field, but many other research groups have made important contributions. It is useful to identify simple structure–property relationships, although the factors influencing two-photon absorption are strongly interdependent, and it is not possible to completely disentangle them. A proper understanding of two-photon absorption in any chromophore requires a consideration of resonances with one-photon transitions (see Section 2), but unfortunately it is often not possible to consider these factors when identifying general trends. Below we use a small number of examples to illustrate the main factors influencing the strength of 2PA in organic dyes. A more comprehensive account of multiphoton dyes can be found in several recent reviews.[14]

4.1.1. Choice of Terminal Groups

4.1.1.1. Terminal Donors

Dialkyl and diaryl amino groups are the most widely used terminal donor groups. Oxygen-based donors (-OR) are generally less effective; for example, compound **7** has a 2PA

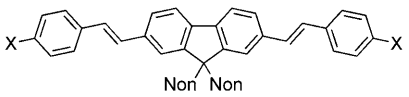

7, X = OMe, δ = 110 GM at 705 nm (fs-TPEF)
8, X = NBu_2, δ_{max} = 1300 GM at 740 nm (fs-TPEF)

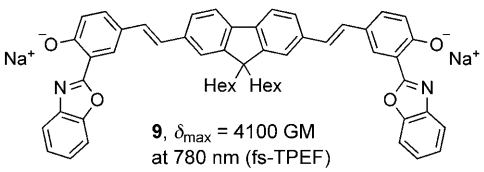

9, δ_{max} = 4100 GM at 780 nm (fs-TPEF)

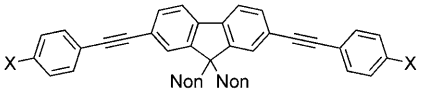

10, X = $NHex_2$, δ = 1200 GM at 705 nm (fs-TPEF)
11, X = SO_2CF_3, δ = 83 GM at 705 nm (fs-TPEF)

cross-section of 110 GM, which is ten times less than that of its nitrogen counterpart **8** (1300 GM).[47] This observation correlates with the Hammett coefficients ($\sigma_p^+ = -1.7$ for $-NMe_2$ compared to $\sigma_p^+ = -0.78$ for $-OMe$).[49] Diaryl amines seem to be better donors in 2PA dyes (for example, compare **3** and **4**) despite their weaker electron-donating ability ($\sigma_p^+ = -1.4$ for $-NPh_2$), but this can be attributed to their greater number of π electrons. As expected, phenoxides are very strong donors ($\sigma_p^+ = -4.27$ for $-O^-$) and give high 2PA cross-sections, for example, compare **9** with **7** and **8**.[50]

4.1.1.2. Terminal Acceptors

A wide range of electron-accepting terminal groups have been investigated,[14,24,47] including many π-deficient heterocycles. However, it seems that D-π-D and D-π-A-π-D structures are generally more effective than A-π-A and A-π-D-π-A systems, as illustrated by comparing compounds **10** and **11**.[47]

4.1.2. Central Bridges and Cores

There are four main parameters to consider when comparing π-conjugated bridges: 1) the donor/acceptor character of the bridge, 2) its size (number of π electrons), 3) its conformation (rigid or flexible), and 4) the nature of the linkers (alkene or alkyne units).

4.1.2.1. Donor/Acceptor Properties of the Central Bridges and Cores

Modification of the central bridge, by increasing its donating or accepting ability, is a widely explored approach to tuning 2PA properties. Attaching electron-withdrawing nitrile groups to the central core increases the δ value by a factor of three in going from **12** to **13**, [24,40] and by a factor of five from **14** to **15**.[51]

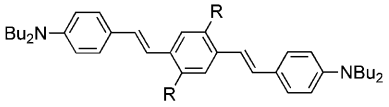

12, R = H, δ_{max} = 640 GM at 725 nm (fs-TPEF)
13, R = CN, δ_{max} = 1700 GM at 830 nm (fs-TPEF)

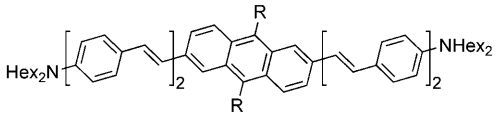

14, R = H, δ_{max} = 1100 GM at 800 nm (fs-TPEF)
15, R = CN, δ_{max} = 5500 GM at 980 nm (fs-TPEF)

Squaraine dyes are another class of chromophore with an electron-accepting core. Compounds **16**[52] and **17**[41] exhibit significant 2PA. In the extreme, carbocations could be regarded as the best electron acceptors, and porphyrin dimers with carbocation cores have recently been shown to exhibit very strong 2PA.[53]

As mentioned in Section 4.1.1.2, chromophores of the type D-π-A-π-D with electron-deficient cores generally

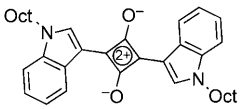

16, δ = 450 GM
at 730 nm (fs-TPEF)

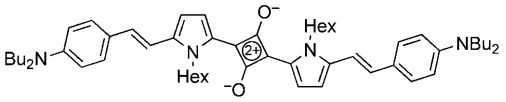

17, δ_{max} = 27 000 GM at 960 nm (fs-z-scan)

exhibit stronger 2PA than comparable A-π-D-π-A structures. It may be that systems with highly electron-rich cores have not yet been thoroughly investigated because they tend to be less stable than electron-deficient ones in normal aerobic environments.

4.1.2.2. Length of the π System

The size of a chromophore (as measured by the number of π electrons N_e)[54] has a strong effect on two-photon absorption (see Section 2.4). Since 2PA cross-sections are molecular quantities, linking together two chromophores in a way that results in no electronic delocalization will simply double the 2PA cross-section ($\delta \propto N_e$). However, if the π systems are strongly coupled, the 2PA cross-section will increase more strongly with N_e as a result of the increase in the transition dipole moments μ_{ig} and μ_{if}. When comparing δ values of chromophores with different numbers of π electrons, it is useful to consider the ratio δ/N_e.

Squaraine dyes **16** and **17** illustrate the huge increase in the 2PA cross-section that can result from increasing the length of a chromophore; they have normalized cross-sections (δ/N_e) of 20 and 750 GM per π electron, respectively. The exceptionally high 2PA cross-section of **17** reflects a small detuning energy $E_{gi}-h\nu$, high transition dipole moments μ_{if} and μ_{ig}, and a narrow line width [small Γ in Eq. (2), Section 2.1]. Part of the difference between the values reported for these two compounds may also reflect the different measurement techniques.

The dependency of the δ value on the length is illustrated nicely by the series of compounds **3**, **12**, **18**, **19**, and **20**[44] (Figure 6); the ratio δ/N_e increases rapidly for the first three compounds, then saturates as the length of the molecule exceeds the π-delocalization length.

The variation of δ/N_e with N_e was also investigated for butadiyne oligomers **21**–**25**. The porphyrin dimer **22** has a cross-section per porphyrin unit of 4500 GM, which is 200-fold greater than that of monomer **21**.[32] Increasing the length of the oligomer to the tetramer **23** (5500 GM per porphyrin), octamer **24** (4600 GM per porphyrin), or polymer **25** (6400 GM per porphyrin) results in little improvement of the 2PA cross-section per porphyrin ring.[28]

A further example of the variation of δ/N_e with N_e is provided by the meso,β-fused porphyrin oligomers **26**–**30** (Figure 7).[55] Again these oligomers show a huge increase in the δ/N_e ratio from monomer to dimer and this ratio continues to increase up to the pentamer, but by smaller increments for each additional porphyrin ring. Even higher 2PA cross-sections have been reported for β,meso,β-fused porphyrin

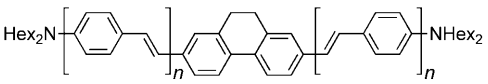

18, $n = 1$, $\delta = 1700$ GM at 740 nm (fs-TPEF)
19, $n = 2$, $\delta = 3300$ GM at 740 nm (fs-TPEF)

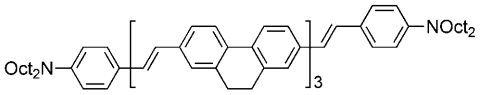

20, $\delta = 3800$ GM at 740 nm (fs-TPEF)

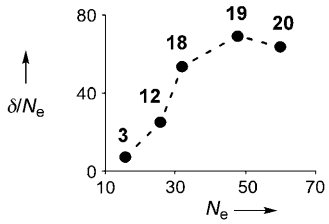

Figure 6. The normalized 2PA cross-sections (δ/N_e) for **3**, **12**, **18**, **19**, and **20** showing the saturation of δ/N_e in the longer π systems.[24,36,44]

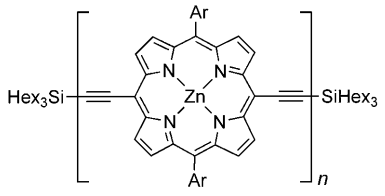

21, $n = 1$, $\delta_{max} = 20$ GM at 850 nm (fs-TPEF)
22, $n = 2$, $\delta_{max} = 9100$ GM at 890 nm (fs-TPEF)
23, $n = 4$, $\delta_{max} = 22\,000$ GM at 960 nm (fs-TPEF)
24, $n = 8$, $\delta_{max} = 37\,000$ GM at 980 nm (fs-TPEF)
25, $n \approx 13$, $\delta_{max} = 83\,000$ GM at 980 nm (fs-TPEF)

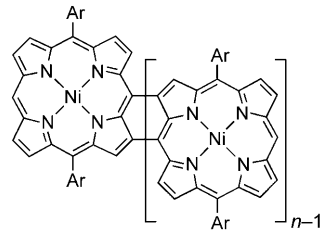

26, $n = 1$, $\delta < 100$ GM at 800 nm (fs-z-scan)
27, $n = 2$, $\delta = 8000$ GM at 1400 nm (fs-z-scan)
28, $n = 3$, $\delta = 17000$ GM at 1700 nm (fs-z-scan)
29, $n = 4$, $\delta = 30000$ GM at 1900 nm (fs-z-scan)
30, $n = 5$, $\delta = 41000$ GM at 2100 nm (fs-z-scan)

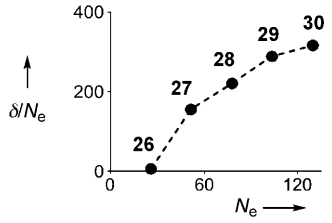

Figure 7. Normalized 2PA cross-sections for porphyrin oligomers **26**–**30**.[55]

oligomers.[56] It is difficult to obtain reliable δ values for these compounds because their 1PA spectra extend far into the near-infrared region; however, recent *z*-scan measurements give $\delta = 41\,000$ GM for the fused porphyrin tetramer at 2300 nm, where there is negligible linear absorption.[57]

4.1.2.3. ***Conformation***

Electronic coupling is optimized when a π system adopts a planar geometry, thereby maximizing π-orbital overlap, so two-photon absorption is sensitive to the conformation of the central π bridge. For example, comparison of **31** (with a

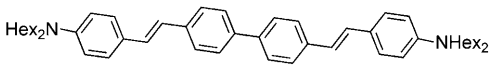

31, $\delta = 1000$ GM at 730 nm (fs-TPEF)

flexible biphenyl bridge)[47] with **8** or **18** (with rigid fluorene and dihydrophenanthrene bridges, respectively) shows that fixing the conformation of the biphenyl unit increases the δ value by about a factor of 1.3–1.7.

A beautiful illustration of the influence of the dihedral angle on 2PA cross-sections was reported by Osuka, Kim, and co-workers for meso-linked porphyrin dimers **33**–**38**.[56] The

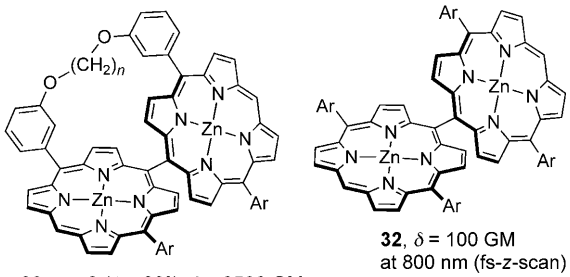

32, $\delta = 100$ GM
at 800 nm (fs-z-scan)

33, $n = 6$ ($\theta = 80°$), $\delta = 3500$ GM
34, $n = 5$ ($\theta = 77°$), $\delta = 3900$ GM
35, $n = 4$ ($\theta = 71°$), $\delta = 4800$ GM
36, $n = 3$ ($\theta = 48°$), $\delta = 6100$ GM
37, $n = 2$ ($\theta = 42°$), $\delta = 6300$ GM
38, $n = 1$ ($\theta = 36°$), $\delta = 7500$ GM
} at 800 nm (fs-z-scan)

mean dihedral angle θ between the two porphyrin π systems (estimated by molecular mechanics calculations) was adjusted by changing the length of a "strap" between the two macrocycles. UV/Vis spectroscopic studies have shown that shortening the strap increases the planarity and rigidity of the dimer, thereby resulting in greater conjugation. In the parent dimer **32**, with no strap, the porphyrin rings are essentially orthogonal ($\theta \approx 90°$, $\delta = 100$ GM), and decreasing this angle to 80° results in a 35-fold increase in δ (**33**, 3500 GM). The largest two-photon cross-section was 7500 GM for **38**, which is similar to the values for conjugated porphyrin dimers **22** and **27**.

Conformational control can also be achieved by self-assembly. Restricting the free rotation of conjugated porphyrin oligomers enhances the electronic communication and so increases the 2PA cross-section. The formation of rigid double-strand ladder complexes of butadiyne-linked oligom-

ers **39**–**42** with 4,4′-bipyridyl) results in a dramatic increase in the 2PA cross-section to around 1300 nm from the butadiyne-coupled oligomers **22**–**25**.[28] A comparison of the conjugation

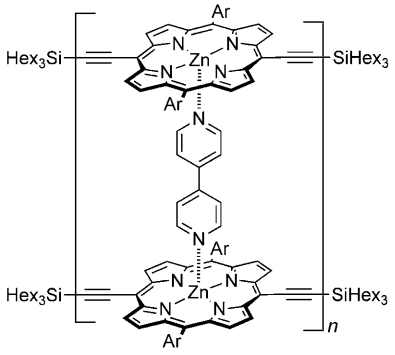

39, $n = 2$, δ_{max} = 13 000 GM at 880 nm (fs-TPEF)
40, $n = 4$, δ_{max} = 18 000 GM at 1305 nm (fs-TPEF)
41, $n = 8$, δ_{max} = 98 000 GM at 1315 nm (fs-TPEF)
42, $n \approx 13$, δ_{max} = 230 000 GM at 1325 nm (fs-TPEF)

signatures S_C [see Eq. (5), Section 2.4] for **39**–**42**, shows that $S_C \propto N_e^4$ for the double strands up to the tetramer **40**, thus indicating that there is complete π delocalization over all four porphyrin units. There is a weaker dependence of S_C on N_e in the corresponding single-strand oligomers **22**–**25**. However, Wasielewski, Kim and co-workers[58] showed that while the formation of a double strand enhances the 2PA cross-section of a conjugated porphyrin trimer, surprisingly formation of a triple strand, by using a tridentate ligand, has the opposite effect. It appears that 2PA in these arrays is still not well understood.

4.1.2.4. Comparison of Vinylene (sp^2) and Ethynylene (sp) Bridges

In general, ethynylene-linked (-C≡C-) systems are less conjugated than the corresponding vinylene-linked (*trans*-CH=CH-) systems, because there are π–π and π*–π* energy mismatches at C(sp^1)–C(sp^2) connections, and because alternation of the bond length is greater with acetylenes.[59] However, this has little effect on 2PA; for example, the δ value of **8** is only 5% greater than that of **10**, and that of **31** is only 15% greater than that of **43**. (The experimental error in the determination of the δ value is about 10%.[47])

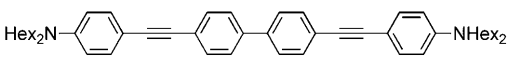

43, δ = 890 GM at 705 nm (fs-TPEF)

When steric congestion is an important issue, as in meso-linked porphyrins,[60,61] acetylenic systems tend to be more conjugated, because, unlike a vinylene linker, an acetylene cannot twist out of conjugation. For example, Rebane, Spangler, and co-workers showed that the vinylene-linked porphyrin **44** has a lower cross-section than the ethynylene-linked porphyrin **45**.[62]

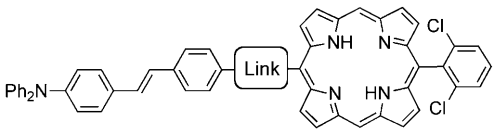

44, link: , δ_{max} = 560 GM at 914 nm (fs-TPEF)
45, link: , δ_{max} = 730 GM at 820 nm (fs-TPEF)

Ethynylene and vinylene linkers have also been compared in porphyrin dimers. The ethynylene-linked dimer **46** shows a 400-fold increase in 2PA cross-section when compared to the

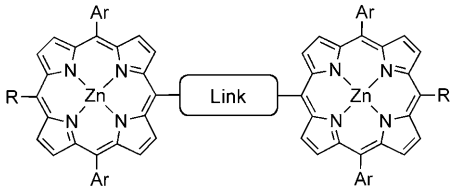

46, link: , R = H, δ_{max} = 8200 GM at 820 nm (fs-TPEF)
47, link: , R = Ph, δ_{max} = 60 GM at 975 nm (fs-TPEF)
48, link: , R = H, δ_{max} = 5500 GM at 830 nm (fs-TPEF)
49, link: , R = , δ_{max} = 17 000 GM at 916 nm (fs-TPEF)

parent monomer.[32,63] Changing the central bridge to vinylene in **47**[64] disrupts the communication between flanking porphyrin rings, and significantly reduces the two-photon cross-section (60 GM). The crystal structure of **47** confirms that the π system is twisted (the C-CH=CH-C bridge makes an angle of 45° to the mean plane of each porphyrin). However, the low 2PA cross-section measured for **47** also reflects its broad one-photon absorption band, which limits the accessible window for TPEF measurements. Changing the ethynylene bridge in **46** to a butadiyne unit to give **48**, slightly reduces the 2PA cross-section, despite increasing the length of the π system.[32,63] Extending π systems by adding acetylene terminal groups to form **22** increases the 2PA cross-section (see Section 4.1.2.2). A further enhancement in the δ value is achieved in dimer **49** by adding electron-withdrawing terminal groups (δ_{max} = 17 000 GM; 8800 GM per porphyrin, δ/N_e = 240 GM).[65] This compound is a promising lead structure for two-photon excited photodynamic therapy (Section 5.6).

4.2. Two-Dimensional Chromophores

4.2.1. Porphyrins and Expanded Porphyrinoids

Large, π-conjugated macrocycles, such as porphyrins, are good candidates for two-photon dyes because of their high transition dipole moments. Most simple porphyrin monomers show small 2PA cross-sections (< 50 GM),[33,66] although a high δ value has been reported for porphycene **50**,[67] an isomer of tetraphenylporphyrin. Very high δ values can be

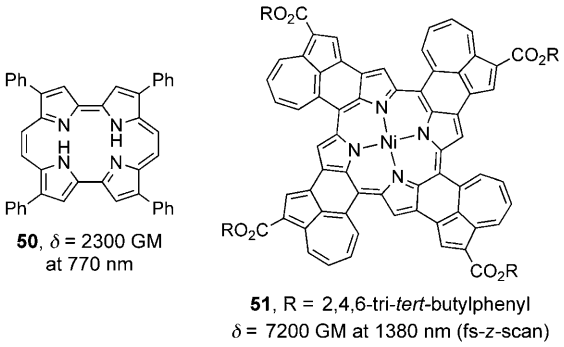

achieved in conjugated porphyrin arrays (see Section 4.1.2.2).[68] Two-dimensionally extended porphyrin π systems also display strong 2PA, as illustrated by azulene-fused system **51** developed by Osuka and co-workers.[69]

Expanded porphyrin analogues have been reported to exhibit strong 2PA. Ahn et al. have compared the δ values for two types of hexaphyrin:[70] [26]hexaphyrin(1.1.1.1.1.1) **52**

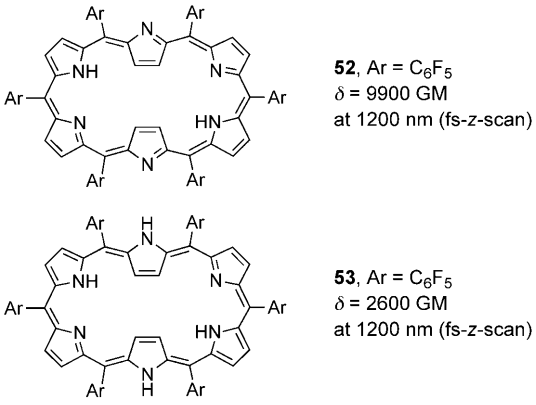

with $\delta/N_e = 260$ GM per π electron exhibits a value comparable to oligomeric porphyrins, while a two-electron reduction of the macrocycle to form [28]hexaphyrin(1.1.1.1.1.1) **53** reduces the δ value by a factor of four. This observation suggests a relationship between the aromatic (**52**) or antiaromatic (**53**) character of the molecule and its 2PA. Osuka, Kim, and co-workers have extended the family of expanded porphyrins and confirmed that aromatic macrocycles generally give higher 2PA cross-sections than non-aromatic ones (as illustrated by octaphyrin complexes **54** and **55**; Figure 8).[71]

Spectacularly high two-photon cross-sections have also been reported for a core-modified hexaphyrin.[72] However, these results come from *z*-scan measurements with a high repetition rate (50 MHz) in a spectral region with appreciable one-photon absorption, so the apparent 2PA cross-section is difficult to interpret. Together, these findings suggest that expanded porphyrins, heteroporphyrins, and other porphyrin analogues are an exceptionally promising class of chromophores for two-photon absorption. Very recently, the 2PA cross-sections of large cyclic oligothiophene macrocycles **56**–

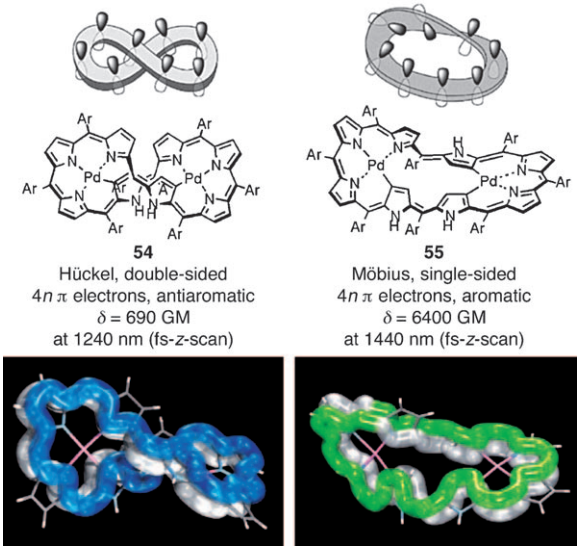

Figure 8. Relationship between geometry and aromaticity: Hückel and Möbius forms of palladium complexes of [36]octaphyrin(1.1.1.1.1.1.1.1) with X-ray structures (adapted from Ref. [71a]).

59 were investigated by Goodson, Iyoda, and co-workers.[73] The absolute values of the 2PA cross-sections increase across the series, but the normalized values (δ/N_e) saturate at compound **57** (Figure 9).

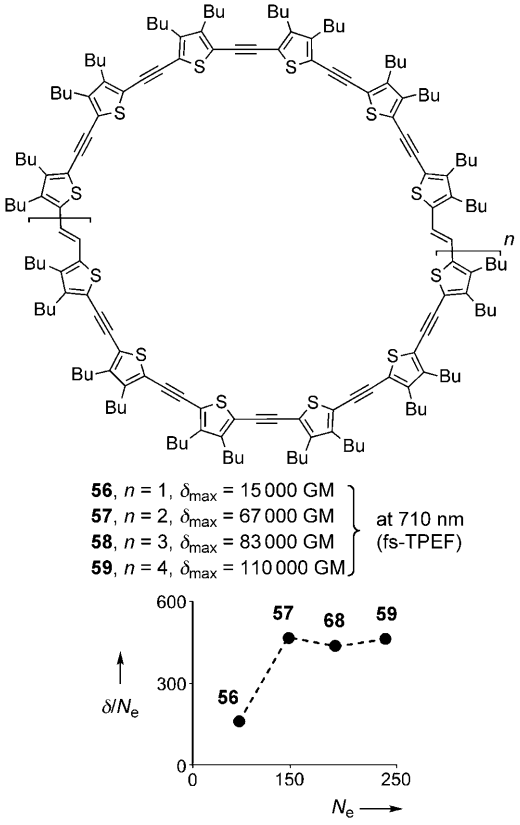

Figure 9. Normalized 2PA cross-section values for cyclic oligomers **56**–**59**.[73]

4.2.2. Branched Planar Chromophores

Trigonal branched octupolar systems form a separate group of 2PA-active compounds that have been widely explored in parallel with linear dipolar and quadrupolar chromophores. If the electronic coupling between the branches is weak, the cross-section increases linearly with the number of branches, but in some cases a much steeper increase in the δ value is observed. The first branched 2PA dyes were reported by Prasad and co-workers in 1999.[42] They tested the influence of branching by linking previously characterized dyes to a central π-conjugated core such as a triphenylamine to give **60**–**62** (Figure 10). They observed a

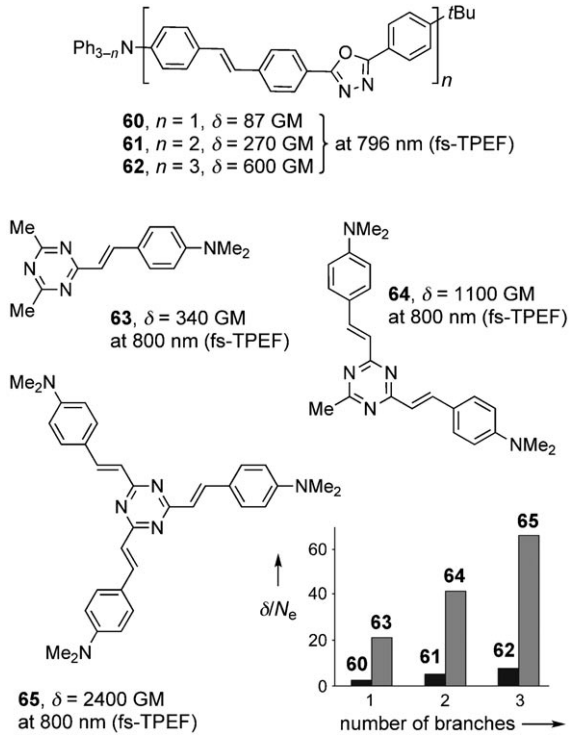

Figure 10. Normalized δ values for the compound series **60**–**62** and **63**–**65**.[42,74]

non-additive increase in the two-photon absorption cross-section. The normalized values for the series (**60**, $\delta/N_e = 3.9$; **61**, $\delta/N_e = 8.2$; **62**, $\delta/N_e = 13$) demonstrate a cooperative enhancement of the 2PA efficiency.

Electron-deficient triazine cores have also been used with electron-rich side arms (**63**–**65**).[74] An improvement in the 2PA cross-section was observed, with a cooperative trend (1:3.3:7.0 for **63**→**64**→**65**)). The normalized values show that electron-donating branches with an electron-poor core (**63**–**65**) give greater 2PA than the inverse system (**60**–**62**) (Figure 10).

The annulenes **66**–**68**, reported by Haley, Goodson, and co-workers,[75] provide another clear example of cooperative enhancement ($\delta/N_e = 0.4$, 7.2, and 17 for **66**, **67**, and **68**, respectively). Although there is a strong increase in the

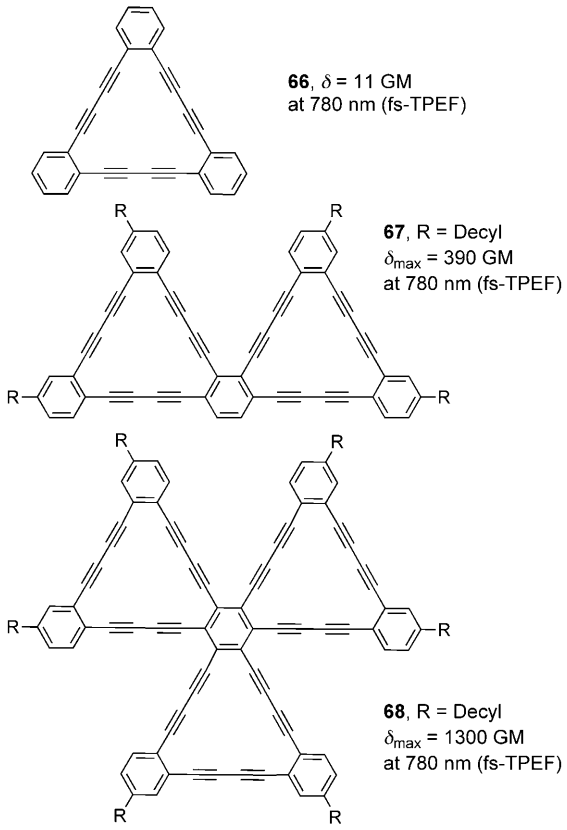

δ value with the number of branches, the normalized values are modest.

4.2.3. Dendrimers

Dendrimers constructed from conjugated chromophores have been widely explored because of their potential application in nonlinear optics, as artificial light-harvesting systems, in light-emitting diodes, and for biological imaging. Drobizhev et al. have reported the photophysical characterization of dendritic chromophores **69**–**71** (Figure 11) based on *trans*-stilbene.[76] It is interesting to compare these dendrimers with stilbene **4** (Section 4.1). The normalized cross-section (δ/N_e) shows a strong increase for the first generation dendrimer **69** compared to **4**, but then declines for the higher generation dendrimers.

Acetylene-linked dendrimers based on a triarylamine core have been investigated by Blanchard-Desce, Goodson, and coworkers.[48] Their behavior is very similar to that of **69**–**71**; again an increase in the δ/N_e ratio is seen for the first generation followed by saturation for the second.

4.3. Conclusions on Design Strategies, Structure–Property Relationships, and Figures of Merit

The normalized 2PA cross-section δ/N_e (where N_e is the number of π electrons) is a useful figure of merit for comparing two-photon chromophores. Recently, several dyes have been reported with $\delta/N_e > 200$ GM per π electron.

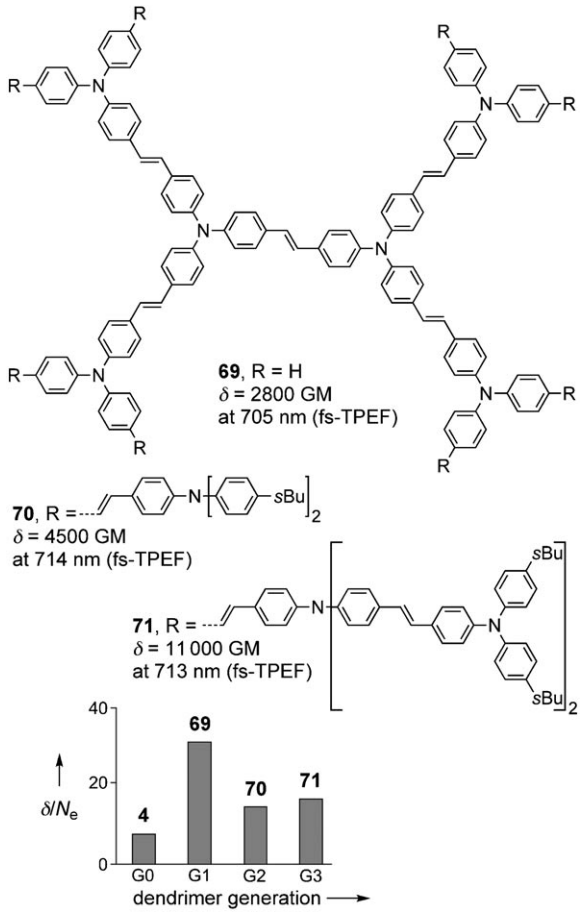

Figure 11. Comparison of normalized 2PA cross-section values for dendrimers **69–71** (the reference compound **4** is included as the zero generation).[33,76]

These chromophores are strikingly diverse, and they originate more from serendipity than from rational design. The classic D-π-A-π-D motif has been explored extensively, and can work well—as in, for example, squaraine **17** ($\delta/N_e = 750$ GM by z-scan), but the presence of donors and acceptors is not essential, as illustrated by the thiophene-acetylene macrocycle **57** ($\delta/N_e = 510$ GM by TPEF). Conformational rigidity and strong π conjugation is a common feature of all these leading 2PA dyes. Conjugated porphyrin oligomers often exhibit strong 2PA, such as butadiyne-linked dimer **49** ($\delta/N_e =$ 240 GM by TPEF), and β,meso-fused pentamer **30** ($\delta/N_e =$ 320 GM by z-scan). Aromatic expanded porphyrin analogues, such as hexaphyrin **52** (Aro6 GM by z-scan), are another important category.

Maximizing the 2PA cross-section is not the only consideration when designing a two-photon dye. It is often useful to pack the maximum effect into the smallest possible chromophore, which is one reason why δ/N_e is such a useful parameter. Sometimes it can be more relevant to divide the δ value by the molecular weight, molecular volume, solubility limit, or maximum achievable number density N of the dye [see Eq. (1), Section 2). Molecular weight is a critical factor for biological dyes, for rapid delivery across membranes. The relevant figures of merit and design criteria depend on the target application (see Section 5).

Most applications use two-photon excitation to activate a spacially localized function. A useful figure of merit is the factor $\delta\Phi$, the product of the 2PA cross-section and the quantum yield Φ for the function of interest (fluorescence, initiation of polymerization, generation of singlet oxygen, or photochemical activation of a drug). The energy and lifetime of the excited state generated by 2PA is an important consideration, because it can influence this quantum yield. Large and strongly conjugated chromophores tend to have small S_1-S_0 energy gaps, and rapid S_1-S_0 nonradiative internal conversion. Such low-energy short-lived excited states may not be useful for fluorescence or photochemical activations. Porphyrin dimer **49** illustrates this compromise: it has fairly high quantum yields for fluorescence and the generation of singlet oxygen ($\Phi_F = 0.10$ and $\Phi_\Delta = 0.70$, respectively, in methanol);[65] longer and more strongly coupled conjugated porphyrin oligomers exhibit higher 2PA cross-sections, but dramatically lower quantum yields.[77] Most of the leading two-photon dyes with $\delta/N_e > 200$ GM have such large conjugated π systems that their fluorescence occurs in the near-infrared region at 700–1200 nm. The family of thiophene-acetylene macrocycles such as **56** (fluorescence: λ_{max} 603 nm, $\Phi_F = 0.08$) is an interesting exception to this trend; they are the only chromophores listed above with $\delta/N_e > 200$ GM to fluoresce in the visible range.

5. Applications of Two-Photon Excitation

5.1. Optical Principles

The differences between one- and two-photon excitation can be appreciated by considering a confocal fluorescence microscope (Figure 12). The optics of this instrument are designed to both irradiate and collect emitted light from a

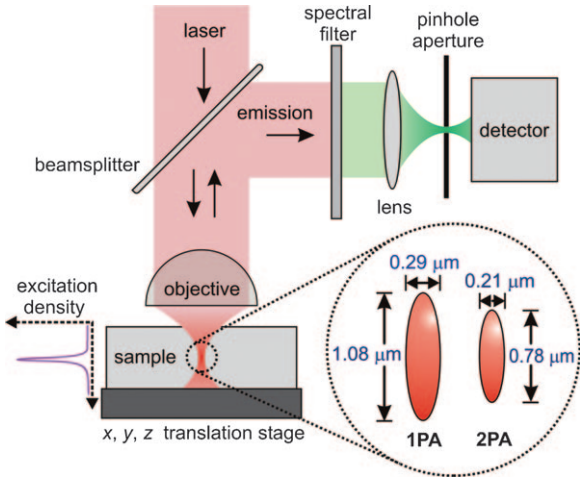

Figure 12. Diagram of a confocal fluorescence microscope. A pulsed infrared laser beam is tightly focused in the sample with 2PA $\propto I^2$, so excitation is confined to the focal region. Emission therefrom, after spectral filtering, is imaged on, and transmitted by, the pinhole; light from other regions is largely rejected. A 3D image is created by translation of the sample relative to the focus. The insert shows the 50% excitation volumes for 1PA and 2PA, assuming $\lambda = 800$ nm, NA = 1.4.

small volume at the focus of the objective. The focal volume is scanned through the sample to build a map of the emission intensity. If the molecular absorption requires a single photon, the excitation density in the focal region is proportional to the local intensity, whereas the density of two-photon excitation is proportional to the square of the intensity and so falls off rapidly away from the focus. The 2PA excitation volume is therefore smaller and increases the resolution of the microscope. This advantage is exploited not only in fluorescence microscopy,[3,5,6] but also in many other applications (see Sections 5.2–5.8).

5.2. The Focal Volume

A collimated beam of monochromatic light of uniform intensity can be focused to a spot whose diameter is proportional to the wavelength and inversely proportional to the numerical aperture (NA) of the lens.[5,78] The excitation volume can be defined as the ellipsoid within which the density of excitation is more than 50% of that at the center of the focus. The highest resolution (and thus the smallest excitation volume) routinely available is provided by oil-immersion objectives with a NA of 1.4. In this case, the width of the excitation volume at a wavelength of 800 nm is 0.29 μm for 1PA and 0.21 μm for 2PA (see insert in Figure 12). However, the resolution is much poorer in the direction parallel to the beam: the length of the excitation volume is 1.08 μm in the 1PA case, and 0.78 μm in the 2PA case. The excitation density across the focus in the axial and radial directions is plotted for 1PA and 2PA in Figure 13a. The length/width ratio of the excitation ellipsoid is about 3.7:1; this ratio is a realistic lower limit, and it increases sharply as the NA of the objective decreases.

The intensity at axial distances greater than 1 μm from the focus exhibits small periodic fluctuations as a result of interference effects, but its average obeys the inverse square law; at 1.1 μm it is a factor of about 10^2 smaller than at the focal point, while at 10 μm this factor is about 10^4. The corresponding 2PA excitation densities are therefore 10^4 and 10^8 smaller than at the focus, thus making it possible to address a small volume element (voxel) deep within a sample without inducing any significant response in the surrounding material. Figures 13b and 13c show that excitation of a fluorescent dye (fluorescein) by 1PA (at 488 nm) generates a stream of emission along the beam path, whereas 2PA (at 960 nm) gives a sharp point of emission at the focus. In Figure 13b, the concentration of the dye is so high that most of the 1PA occurs before the light reaches the focus. Under more dilute conditions the one-photon excited emission would be hour-glass shaped.

5.3. Advantages of Two-Photon Excitation

The size of the focal volume is proportional to the wavelength and, because the contraction in the excitation volume achieved by going from 1PA to 2PA is less than a factor of two (see insert in Figure 12, or Figure 13a), the resolution achieved from 2PA at 800 nm will be less than that from 1PA at 400 nm. However, two factors give 2PA a decisive advantage: 1) the sample will invariably have much larger absorption and scattering losses at the shorter wavelength, and short-wavelength irradiation often causes photochemical damage in biological samples, and 2) the much sharper contrast in the excitation density prevents the occurrence of parasitic emission or photochemical conversion outside the focal volume.[5] Figure 14 illustrates the spatial

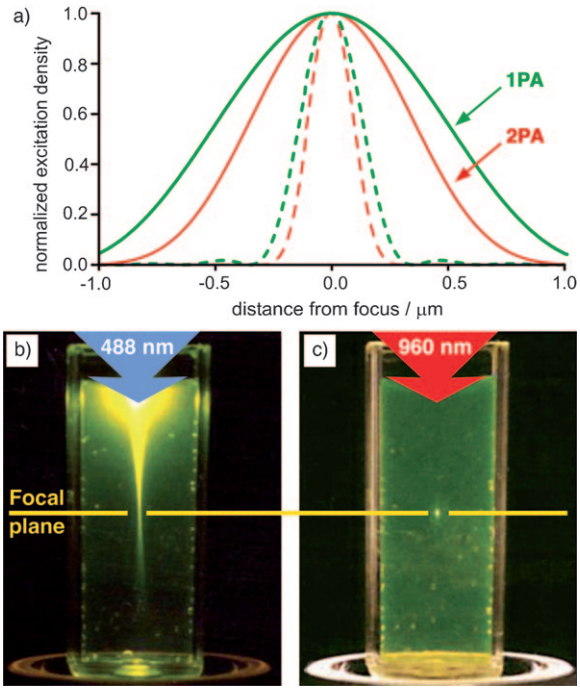

Figure 13. a) Excitation density as a function of axial and radial distance from the focal point (green: 1PA; red: 2PA; solid line: axial, dashed line: radial; NA = 1.4, λ = 800 nm). Localization of the excitation of fluorescein: b) single-photon excitation by focused light (488 nm; 0.16 NA); c) two-photon excitation using focused (0.16 NA) femtosecond pulses of 960 nm light. Parts (b) and (c) reproduced from Ref. [5] with permission.

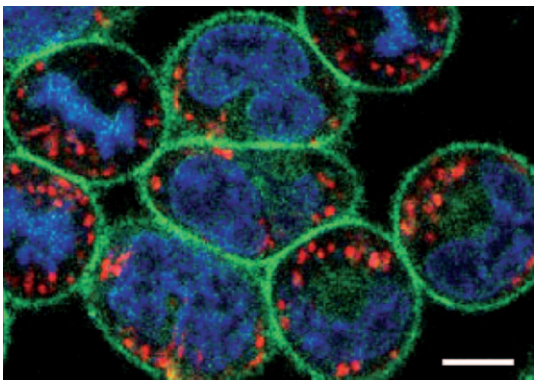

Figure 14. Two-photon confocal microscope images of fibroblast cells using fluorescent stains for DNA (blue; 4′,6-diamidino-2-phenylindole, DAPI), plasma membranes (green; PATMAN), and mitiochondria (red; tetramethylrhodamine). Scale bar: 5 μm. Reproduced from Ref. [5] with permission.

and spectral resolution obtainable in a confocal microscope under two-photon excitation in a specimen of stained fibroblast cells.[5]

5.4. Tracers, Probes, and Sensors

In their simplest incarnations, 2PA dyes have been used as tags to track the migration of nonfluorescent drugs inside cells. For example, Prasad and co-workers employed a D-π-A stilbene dye to trace the cellular pathway by which a chemotherapeutic doxorubicin conjugate enters and localizes within human breast cancer cells.[79] Recently, TPEF stains have been developed for specific subcellular structures and organelles.[80] The most important parameter for these dyes is their brightness ($\Phi_F\delta$): the product of their 2PA cross-section (δ) and their fluorescence quantum yield (Φ_F). Probe **72** has

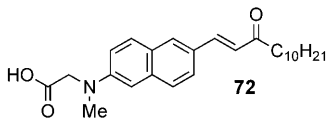

72

$\Phi_F\delta$ = 80 GM at 800 nm in hydrophobic liposomes

$\Phi_F\delta$ = 10 GM at 800 nm in hydrophilic liposomes

been employed to visualize lipid rafts in live tissues by using two-photon microscopy. It displays an eightfold enhancement in brightness when encapsulated in hydrophobic liposomes ($\Phi_F\delta = 80$ GM) as compared to hydrophilic liposomes ($\Phi_F\delta =$ 10 GM).[80a] The main reason for this is a change in Φ_F rather than a change in δ.

Several two-photon dyes have been designed to exhibit TPEF that is sensitive to the concentrations of metal cations or anions as well as to changes in the pH value. In most cases, coordination to the analyte changes the electron-donating nature of the terminal group of the dye. Nearly simultaneous publications by the research groups of Marder[81] and Cho[82] reported aza-crown ethers where the nitrogen atom of the macrocycle acts as the donor in a D-π-A-π-D chromophore. The complexation of Mg^{2+} to **73** brings about a 50-fold

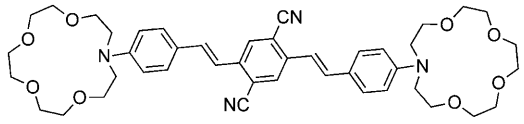

73, δ_{max} = 2200 GM at 810 nm (fs-TPEF), Φ_F = 0.20
Mg^{2+}·**73**, δ = 45 GM at 810 nm (fs-TPEF), Φ_F = 0.19

reduction in the δ value at 810 nm (presumably by reducing the donor strength of the lone pair of electrons on the nitrogen atom) while not affecting the fluorescence quantum yield.[81]

Recent work has focussed on designing highly selective two-photon sensors for specific metal cations, and of these zinc chelators have received the most attention. In some cases, fluorescence is suppressed by cation binding,[83,84] whereas in others chelation enhances both the δ and Φ_F values.[86,87] For example, in **74**[85] coordination of the pyridine ring at the end of the chromophore to Zn^{2+} makes this substituent a better electron acceptor, thereby enhancing the δ value. This approach has been extended to chelators for heavy-metal cations including mercury[88] and cadmium,[89] and to fluoride anions.[90] Sensitive 2PA pH probes have also been developed by using the same principle.[91]

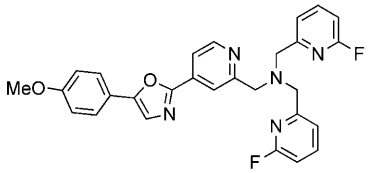

74, δ_{max} = 31 GM at 690 nm (fs-TPEF), Φ_F = 0.35
Zn^{2+}·**74**, δ_{max} = 77 GM at 730 nm (fs-TPEF), Φ_F = 0.71

5.5. Photoactivation and Drug Delivery

Two-photon-initiated release (uncaging, that is, deprotection) of bioactive molecules is an extremely powerful tool for fundamental research in the life sciences. Neurophysiologists are especially interested in controlling neuronal circuits by achieving rapid, localized release of neurotransmitters, proteins, and ions. Compared to the dyes discussed in Section 4, the chromophores currently used for the uncaging have extremely small 2PA cross-sections. These δ values are often determined by measuring the amount of femtosecond two-photon excited photochemical products (fs-TPEPP); this method is analogous to fs-TPEF (Section 3.2). The majority of the dyes used for two-photon uncaging have been adopted from traditional one-photon microscopy and have not been optimized for nonlinear excitation. The neurotransmitter glutamine is the most widely used 2PA-activated caged compound. The 4-methoxy-7-nitroindolino glutamate derivative has led to considerable advances in understanding neuronal signaling, despite its extremely small 2PA cross-section (0.06 GM).[92,93] Photolabile masked glutamates, based on coumarin (**75**, Scheme 1)[94] and stilbene[95] dyes, with larger δ values have been explored. The 2PA-initiated release of calcium is also vital for analyzing molecular processes at single synapses. To date, the most promising caged calcium compound **76** has a 2PA cross-section of just 0.6 GM.[96] Another interesting example of two-photon-initiated release is the neurotransmitter NO from a nitrosyl complex, as reported by Ford and co-workers.[97] Here a porphyrin serves as an intramolecular antenna to sensitize a metal cluster.

Encapsulation in micelles and lipsomes is a widely used strategy for drug delivery. If the stability of the construct can be controlled by 2PA, then high local concentrations of an active compound can be released selectively in diseased tissues. The first demonstration of a micellular system which degrades after 2PA was reported by Fréchet and co-workers,[98] who used a synthetic micelle produced from **77** (Scheme 2). This diazocompound undergoes a Wolff rearrangement upon optical excitation, thereby increasing its hydrophilicity and destroying the micelle.

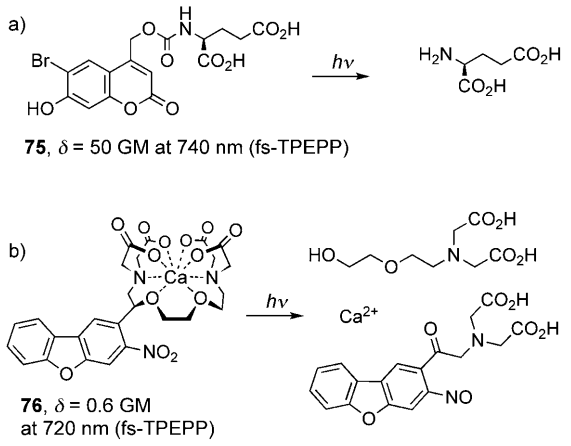

Scheme 1. Two examples of two-photon-excited photoactivation: a) uncaging of glutamatic acid[94] and b) uncaging of calcium.[96]

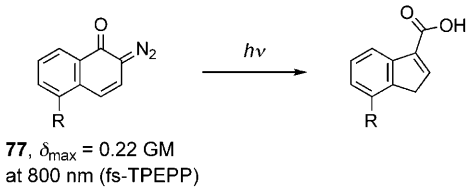

Scheme 2. This two-photon-excited Wolff rearrangement of **77** ($R = SO_2NH(CH_2)_{11}CO_2(CH_2CH_2O)_{17}C_2H_5$) gives a hydrophilic product which leads to micelle disintegration and guest release.[98]

5.6. Photodynamic Therapy

The benefits that 2PA brings to microscopy also translate to photodynamic therapy (PDT).[99] One-photon PDT is widely used to treat cancers of the skin and hollow organs, as well as the eye disease macular degeneration. PDT employs a photosensitizer, which is harmless in the absence of light, to induce damage upon optical irradiation. The phototoxicity of these photosensitizers is primarily due to singlet oxygen, which is generated by energy transfer from the excited state of the sensitizer to molecular oxygen. The quantum yield Φ_Δ for the generation of singlet oxygen is a key parameter for drug prototypes. Two-photon PDT should confine excitation of the photosensitizer to the focal volume. The longer-wavelength (near-IR) light required for two-photon excitation also penetrates deeper into living tissues than visible light. These advantages make 2PA PDT of particular interest in neurology and ophthalmology, where there is a need to improve therapeutic targeting whilst simultaneously minimizing invasiveness.

Two-photon PDT has often been proposed as a means to improve treatment depth and targeting.[100–102] The first conclusive demonstration of 2PA PDT was reported in 1997 by Wachter and co-workers, who used a psoralen-based drug to kill *Salmonella typhimurium* bacteria in vitro.[12] Subsequently, clinically approved porphyrin derivatives have been used to demonstrate two-photon-excited destruction of cultured eukaryotic cells[103] and blood capillaries in chicken embryos.[104] In all these studies, the small 2PA cross-sections of the drugs (<100 GM) necessitated the use of laser powers close to the tissue-damage threshold. Two-photon PDT with these sensitizers is impractical as a clinical treatment: the cumulative effect of scanning the focus through the disease volume would cause indiscriminate photodamage. New photosensitizers with high δ values are needed to allow a significant reduction in irradiation intensities and treatment times, and make 2PA PDT an attractive therapeutic strategy.

A common method for improving the 2PA efficiency of a photosensitizer is to attach two-photon dyes to harvest light and funnel energy to the drug by Förster resonance energy transfer (FRET). Fréchet and co-workers have attached eight "antenna" 2PA dyes to a porphyrin core; the resulting dendrimer was used to demonstrate the production of singlet oxygen through two-photon excitation, although it has not yet been engineered for aqueous solubility or biological evaluation.[105] Intracellular delivery has been achieved for another FRET conjugate **78** by including a peptide (octreate) that

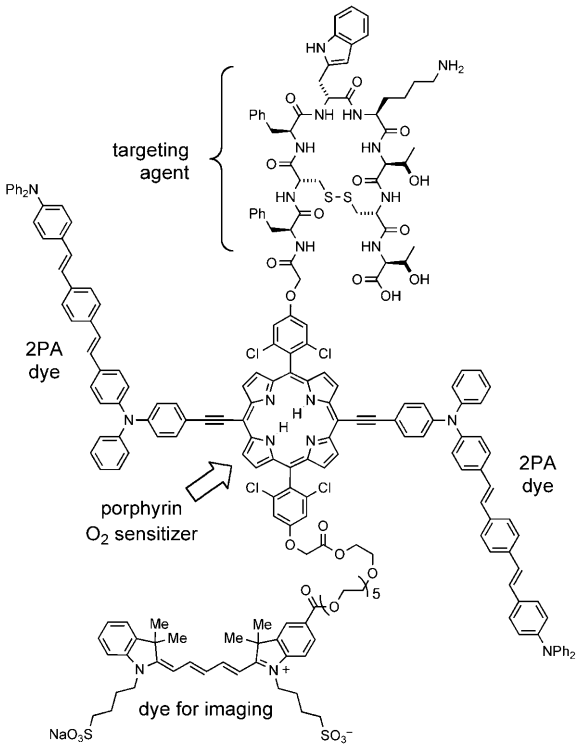

78, δ_{max} = 2200 GM at 820 nm (fs-TPEF)

targets a somastatin receptor commonly over-expressed in human cancer cells.[106] The porphyrin core of **78** is substituted with two distyrylbenzene dyes to improve the 2PA cross-section and a cyanine dye to facilitate fluorescence imaging studies. This construct has been used to demonstrate PDT in highly scattering tissue models. In practice, the photosensitizer and 2PA dye may not need to be covalently bound; co-encapsulation in silica nanoparticles has been shown to induce a phototoxic effect in vitro upon excitation with femtosecond pulsed near-IR light.[107]

The other approach to designing 2PA photosensitizers is to adapt 2PA chromophores that produce singlet oxygen efficiently. For this reason, porphycenes such as **50** and the water-soluble squaraines related to **17**[108] have been proposed for 2PA-PDT.[67] The latter dyes have been shown to accumulate in cultured cells without affecting cell viability. Particular attention has been focused on acetylene-linked conjugated porphyrin dimers, such as **49** (Section 4.1.2.4) and **79**, as the basis for new 2PA drugs. Kobuke and co-workers

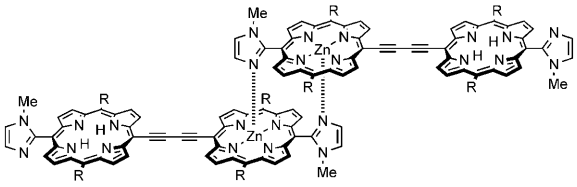

79 (R = $CH_2CH_2CO_2Na$)
80 (R = Oct), δ_{max} = 7600 GM at 887 nm (fs-*z*-scan)

have studied self-assembled imidazolyl porphyrin dimers: coordination to form **80**, a dimer of dimers, gives a twofold enhancement of the 2PA cross-section per porphyrin (δ_{max} = 1900 GM per porphyrin) compared to the disaggregated dimer (δ_{max} = 900 GM per porphyrin). The increased 2PA efficiency is attributed to an enhanced transition dipole moment by exciton coupling between the dimers. The water-soluble derivative **79** has been introduced into cells and induces cell death upon one-photon excitation.[109]

We recently reported a family of hydrophilic, conjugated A-π-D-π-A porphyrin dimers which are nontoxic in the absence of light.[65] Compound **49** (Section 4.1.2.4) is the first drug with a large 2PA cross-section (δ_{max} = 17000 GM) that has been proven to induce a two-photon PDT effect in vivo. Two-photon excitation of **49** selectively occluded arteries (45 μm diameter, Figure 15) in a living mouse, whereas the leading commercial photosensitizer Visudyne was inactive under these conditions. These new compounds represent only the first generation of 2PA PDT photosensitizers. Further optimization is needed, not only to increase their therapeutic efficiencies, but to impart appropriate biodistribution and pharmacokinetic behavior.

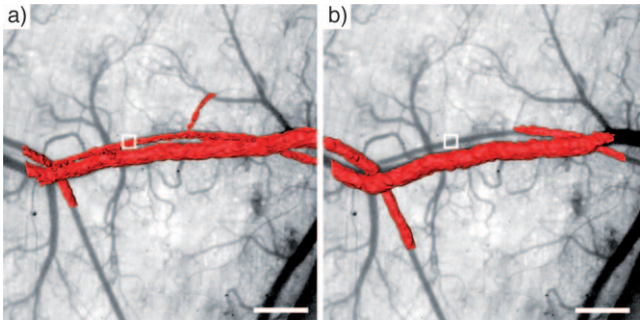

Figure 15. Targeted two-photon-induced arterial closure using the 2PA photosensitizer **49**. Optical Doppler coherence tomography images pre- (a) and post-treatment (b) are overlaid on the pretreatment stereomicroscope image to show blood flow (red). The blood flow in the targeted artery is from left to right. The white boxes indicate the irradiated region (scale bar, 400 μm). Reproduced from Ref. [65] with permission.

5.7. Microfabrication

Two-photon excitation is widely used to fabricate three-dimensional microscopic structures with sub-micrometer resolution.[7] This technique achieves contrast in solubility by using the photoinitiated polymerization or depolymerization reactions that are the basis of many lithographic processes. If a micrometer-sized structure is to be fabricated at a depth of several tens of micrometers, the material above and below the focus will be continuously exposed at low intensity while the focal volume traces out the structure. Single-photon excitation can therefore lead to substantial photochemistry outside the focal volume, with the consequent loss of lithographic contrast and definition. Two-photon microfabrication is a rapidly expanding field of research, and there is only space here to give a brief introduction. Several detailed reviews of this field have been published recently.[7,110,111]

Suitable resists for microfabrication are based on 1) the radical polymerization of acrylates, 2) the acid-catalyzed cationic polymerization of epoxides, and more recently 3) the polymerization of As_4S_6 glasses to give a cross-linked insoluble inorganic framework.[112] Cationic polymerization is usually preferred because radical polymerization can lead to uncontrolled diffusion that lowers the spatial resolution, while also being susceptible to oxygen quenching. In most examples of 2PA microfabrication, the initiators are those established in conventional lithography, and the writing speed is limited by their small 2PA coefficients. Major improvements in fabrication speed are therefore possible by combining a sensitizer with a large 2PA cross-section with an initiator with a high quantum efficiency. An example is compound **81**

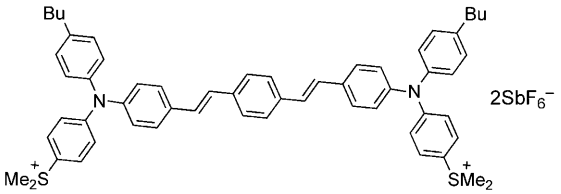

81, δ = 690 GM at 705 nm (fs-TPEF)

(a derivative of **12**, Section 4.1.2.1), in which a quadrupolar 2PA dye is covalently linked to dimethylsulfonium groups.[113] Their proximity ensures efficient electron transfer from the excited state of the dye to the oxidizing sulfonium centers, whose fragmentation leads to the efficient generation of acid.

Two examples of 2PA microfabrication, and confocal imaging, are illustrated in Figure 16.[114,115] In both cases SU-8 epoxy photoresist containing a photoacid generator and an acid-sensitive coumarin dye is used. Excitation of the former creates free acid, which can be mapped by the excitation at 543 nm, because protonation of the coumarin increases its

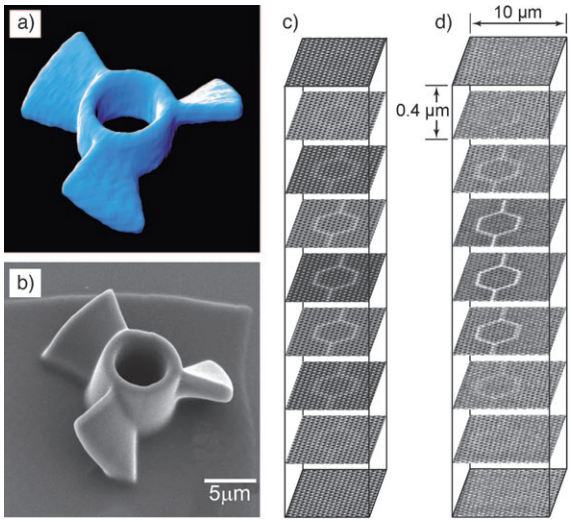

Figure 16. Microfabrication in photoresist resin: a) Confocal fluorescence microscope image of the acid distribution introduced by 2PA writing. b) SEM image of the object obtained by thermal polymerization, followed by development in a solvent that dissolves the unexposed photoresist.[114] c) Simulated target structure and d) confocal micrograph after 2PA writing of waveguide elements into a photonic crystal structure.[115]

absorption at this wavelength (Figure 16a).[114] The sample is then heated and the acid initiates polymerization; after washing, an insoluble material is left in the regions exposed to light. The structure can then be imaged by scanning electron microscopy (SEM, Figure 16b). To produce the structure shown in Figure 16c,d, the sample was initially exposed to a face-centered cubic interference pattern generated by the 1PA of four UV laser beams (355 nm), thereby creating a latent "photonic crystal" with a lattice spacing of 600 nm.[115] Prior to heating, the coumarin fluorescence was used to align a subsequent exposure, and a waveguide structure was added by 2PA activation of the photoacid at 660 nm. The device structure is effectively confined within a thickness of 1.2 μm.

Figure 17 shows a "log-pile" photonic crystal made by 2PA writing in an SU-8 epoxy photoresist, subsequently rendered into silicon by a templating process.[116] The approximatly 300 nm wide lines have a depth of about 1.0 μm when the crystal is viewed in cross-section (Figure 17, bottom left), as expected from the shape of the focal ellipsoid (Figure 12). The solubility of a photoresist is a nonlinear function of the exposure dose, so it is usually possible to arrange for only the maximum intensity in the focal volume to generate insoluble polymer. Thus, it is possible to fabricate objects with smaller dimensions than those suggested by the size of the excitation ellipsoid plotted in Figure 13a. Objects with a width of 65 nm, but much greater depth, have been made in this way, although they are substantially distorted and have poor uniformity.[117]

While the ability to fabricate complex components on a sub-micrometer scale may suggest a wide range of applications, in practice these are limited by the time taken to address and convert the large number of voxels that define a complex object. The intrinsically low 2PA cross-sections and the serial nature of the method mean that typical writing times for a volume of $100 \times 100 \times 100\ \mu m^3$ are of the order of minutes, so that mass production applications are currently unrealistic. It is possible, however, that this problem could be alleviated by well-designed 2PA sensitizers and by advances in laser technology.

5.8. Three-Dimensional Optical Data Storage

Current optical data storage devices, such as CDs and DVDs, use one-photon processes to write and read information on a two-dimensional surface. The tightly localized 2PA excitation volume, and high discrimination against the surrounding background, enables data to be stored in a three-dimensional medium, thereby leading to a huge increase in data density.[8,9] The combination of a two-photon-excited photoacid generator and an acid-activated fluorescent dye (similar to that of Figure 16) has been used to fabricate a prototype data storage disk with hundreds of layers of information within the volume of the medium (Figure 18).[118] This disk had a diameter of 120 mm and a thickness of 1.2 mm, and it was able to record 1 Tbyte of data, which is about 200 times that of a conventional DVD.

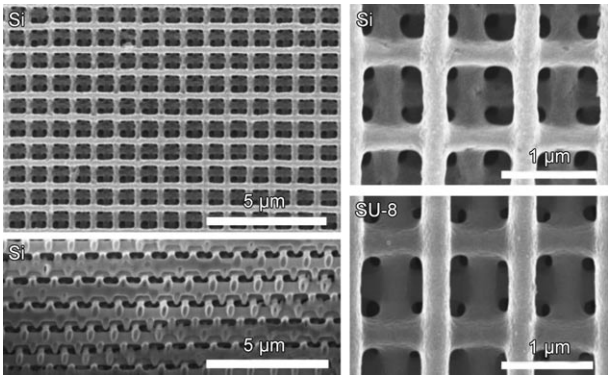

Figure 17. SEM images of a "log-pile" photonic crystal made by 2PA writing in an SU-8 epoxy photoresist, subsequently rendered into silicon by a templating process.[116]

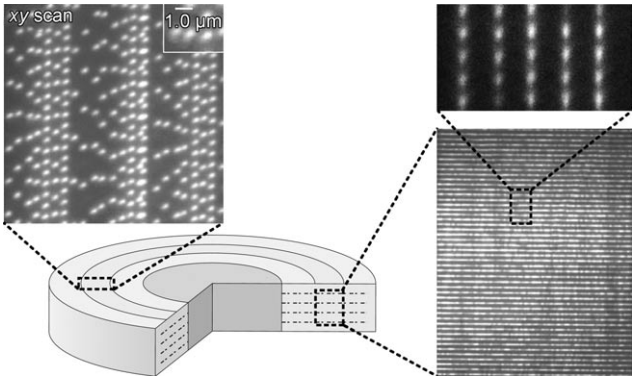

Figure 18. A 3D data storage disk with many layers of information written and read by two-photon excitation. Reproduced from Ref. [118] with permission.

However, the writing speed was only 3 Mbyte s^{-1}, which corresponds to a time of about 4 days for writing 1 Tbyte, thus highlighting the need for more sensitive materials for two-photon excitation. Photochromic dyes with large 2PA cross-sections could be very useful in this area. For example, the photoisomerization of the *trans*-porphyrin-perinaphthothioindigo dye **82** generates a *cis* isomer, which like the

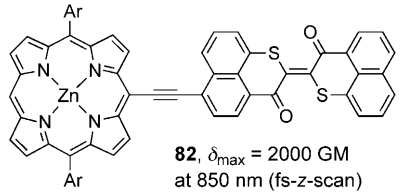

trans isomer is thermally stable at room temperature.[119] The presence of the porphyrin results in the 2PA cross-section being large, thus enabling rapid switching on a timescale approaching that needed for a working memory. Nondestructive readout is, however, not practical in this case, because the excitation spectra overlap and photoisomerization is reversible. A variety of bisthienylethene-based two-photon photochromic dyes have also been developed.[120]

5.9. Optical Power Limiting

The term "optical power limiter" is used to describe a material that exhibits intensity-dependent absorption, such that it is transparent to light at low intensities but opaque to intense light.[10] Such a material behaves like a shutter, responding on an ultrafast (ps to ns) timescale. Optical limiters are "smart materials" in the sense that their function originates from the intrinsic properties of the material, rather than requiring any external control mechanism. For example, Figure 19 shows the optical limiting response of stilbene derivative **3** (Section 4.1) to 5 ns pulses at 600 nm.[36] At low input energies (namely, at low light intensity) 95 % of the light is transmitted ($T = 0.95$), but as the input energy is increased,

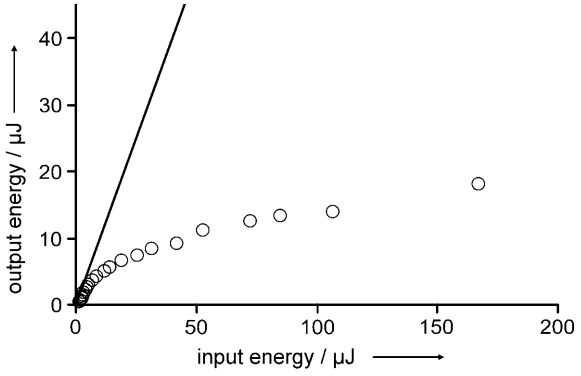

Figure 19. Optical limiting by a two-photon dye 4,4′-bis(dibutylamino)stilbene (**3**, 0.14 M solution in acetone) to 5 ns pulses at 600 nm. The solid line corresponds to a sample with a linear transmittance of $T = 0.95$. Reproduced from Ref. [36] with permission.

the output energy remains below 20 μJ, and most of the light is absorbed. There is a strong demand for optical power limiters that can protect delicate sensors from lasers for military applications. They also have applications in optical telecommunications for removing intensity spikes. There is a particular demand for optical limiters which operate over a broad range of wavelengths to give "frequency-agile" protection.

The main mechanisms for optical-power limiting are excited-state absorption (ESA) and nonlinear scattering. ESA arises when absorption of light generates an excited state (singlet or triplet) that absorbs more strongly than the ground state (Figure 20). Absorption by excited singlet states ($S_1 \rightarrow S_n$) gives an immediate, but short-lived, effect. Absorption from excited triplet states ($T_1 \rightarrow T_n$) grows on a slower timescale (ps to ns), because of intersystem crossing (ISC), and typically decays over a few microseconds. The longer lifetimes of triplet states lead to greater populations of the excited states, for a given light intensity, and lead to a more-sensitive optical power limiter.

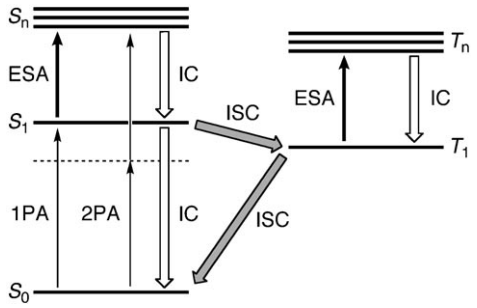

Figure 20. Simplified Jablonski diagram for optical power limiting by either 1PA or 2PA. Shown are the excited-state absorption (ESA), internal conversion (IC), and intersystem crossing (ISC).

2PA would appear to be an ideal mechanism for optical power limiting because (unlike ESA) it requires no linear absorption, so should give excellent transparency at low-intensity light. However, 2PA cross-sections of current materials are not large enough to form effective optical limiters purely by two-photon absorption. A more practical strategy is to use a combination of 2PA and ESA (Figure 20). A small amount of 2PA can generate a concentration of excited states, which then absorb more light by cycling between ESA and internal conversion (IC). Many two-photon dyes exhibit this behavior, and stilbene derivative **3** (Figure 19) is one example.[36] Effective optical limiting requires the following combination of properties at the excitation wavelength: large 2PA cross-section, small 1PA cross-section (that is, low $S_0 \rightarrow S_1$ extinction coefficient), high triplet quantum yield ($S_1 \rightarrow T_1$ ISC faster than $S_1 \rightarrow S_0$ IC), strong ESA, and long triplet lifetime (slow $T_1 \rightarrow S_0$ ISC). In this case, $N\delta$, the product of the 2PA cross-section and the number density of chromophores in the medium (see Section 2.1), is a better figure of merit than δ. It is important that the dye can be used at high concentrations in a solvent or solid-phase host material. Under these conditions phase-

separation can occur, which leads to problems of scattering, and aggregation can broaden the linear absorption bands, which leads to a loss of transparency. It can be difficult to design a dye with the right combination of solubility properties and optical characteristics; sometimes it may be preferable to use a mixture of dyes such that one dye captures light by 2PA and transfers this energy to a second dye exhibiting ESA.[121]

6. Summary and Outlook

Rapid advances in molecular engineering, through the design and synthesis of improved two-photon dyes, are poised to make a significant impact on diverse fields of technology—from engineering and materials science to physiology and medicine. Two-photon excitation is already widely used in optical microscopy and microfabrication, and it promises to bring huge benefits in localized uncaging, drug delivery, and photodynamic therapy as well as 3D data storage and optical power limiting. In most cases, these applications have been demonstrated by using conventional dyes with modest 2PA cross-sections ($\delta < 50$ GM). Recently, many new chromophores have been developed with very high 2PA cross-sections ($\delta > 10\,000$ GM), and there is great scope for translating these systems to practical applications. For example, we have adapted a porphyrin-based dye with $\delta = 17\,000$ GM so that it can be applied as a photosensitizer in photodynamic therapy (PDT). This dye (**49**) has been used to close blood capillaries with high spatial resolution in live mice (Figure 15). Two-photon excitation should bring significant advantages to PDT in areas such as ophthalmology. Other novel medical applications of 2PA are beginning to emerge, such as in cataract surgery.[122]

The widespread use of two-photon fluorescence microscopy has encouraged cell biologists to go beyond imaging, and to monitor and manipulate the local concentrations of bio-active compounds by using 2PA (see Sections 5.4 and 5.5). It is remarkable that these studies have demonstrated a significant advantage by using two-photon excitation, despite the fact that most of this work has used dyes with small 2PA cross-sections, sometimes even less than 1 GM. There appear to be tremendous opportunities for synthesizing improved two-photon probes and uncaging reagents. The need for the dye to pass rapidly through cell membranes favors low-molecular-weight compounds, and so the challenge is to pack a large 2PA cross-section into a small dye. Biosynthetic fluorescent proteins can be incorporated into living systems by genetic manipulation, and often exhibit better photostability than synthetic dyes.[123] The first system of this type was green fluorescent protein (GFP), isolated from jellyfish, but now a wide variety of these dyes have been developed with emission across the visible spectrum. The importance of this approach was recognized by the award of the 2008 Nobel Prize in Chemistry to Shimomura, Chalfie, and Tsien. The δ_{max} value of wild-type GFP is quite low (12 GM at 810 nm), while a mutant known as cyan fluorescent protein exhibits two stronger 2PA bands ($\delta_{max} = 100$ GM at both 550 and 870 nm; fs-TPEF).[5,124] It will be interesting to see whether genetic manipulation can be used to create protein-encapsulated dyes with even larger 2PA cross-sections.

Clear principles for the design of 2PA dyes have been developed, and yet all the best 2PA chromophores still come from serendipitous discoveries (which can often be rationalized retrospectively in terms of transition dipole moments and energy gaps, Section 2), rather than from rational design. There are good theoretical reasons to suspect that centrosymmetric D-π-A-π-D and A-π-D-π-A systems will generally give stronger 2PA than the corresponding dipolar D-π-A chromophores, and this is supported by experimental findings. However, it is important to remember that, for many applications, the energy of the excited states generated by 2PA is crucial for fluorescence or further photochemistry—a large delocalized π system with a high δ value and a very low energy excited state may not be useful. A centrosymmetric dye gains its high δ value from resonance with an intermediate state of roughly half the energy of the final state accessed by 2PA. This final state will relax rapidly to the intermediate (S_1) state, and (by Kasha's rule) most of the fluorescence and photochemical processes will originate from this intermediate state. Thus, when a centrosymmetric dye absorbs two photons, the energy of one of the photons is lost as heat, whereas in a dipolar dye, 2PA occurs at the S_1 state so most of the energy of both the photons can be used for further photochemical processes.

Two-photon excitation has become very widely used in 3D microfabrication, and it has great promise as a method for 3D optical data storage; however these two applications are held back from commercialization by the slow writing speeds, which are a consequence of the low δ values of the current dyes. These applications would benefit from the development of dyes that can be activated by 2PA in the UV or in the blue range (300–500 nm) because short wavelengths lead to higher diffraction-limited resolution. Very few two-photon dyes have as yet been developed for excitation below 500 nm.

Although two-photon excitation of organic dyes has been investigated for about 45 years, most of the advances have been achieved in the last 5–10 years, and the field is still very much in its infancy. We anticipate that it will develop more rapidly during the next 10 years, as it becomes widely appreciated that two photons can be better than one.

Abbreviations

1PA	one-photon absorption
2PA	two-photon absorption
A	electron acceptor
c	speed of light, Eq. (2)
C	a constant in Eq. (4)
CI	configuration interaction
D	electron donor
Dec	n-decyl, $C_{10}H_{21}$
D term	first dipolar term of Eq. (3)
ε_0	vacuum permittivity, Eq. (2)
E_{gi}	energy gap, see Figure 2
ESA	excited state absorption
FRET	Förster resonance energy transfer

fs	femtosecond, 10^{-15} s
GFP	green fluorescent protein
GM	Göppert-Mayer, a unit of 2PA
HOMO	highest occupied molecular orbital
h	Planck constant
Hex	n-hexyl, C_6H_{13}
IC	internal conversion
ISC	intersystem crossing
LUMO	lowest unoccupied molecular orbital
N	number of molecules per unit volume
N_e	number of π electrons within a molecule
Non	n-nonyl, C_9H_{19}
ns	nanosecond, 10^{-9} s
Oct	n-octyl, C_8H_{17}
PDT	photodynamic therapy
ps	picosecond, 10^{-12} s
S_0	singlet ground state
S_1	first excited singlet state
S_C	conjugation signature, Eq. (5)
SEM	scanning electron microscopy
SU-8	a negative-tone epoxy photoresist
S_{fg}	defined in Eq. (2)
T	transmittance
T_1	first excited triplet state
TPEF	two-photon excited fluorescence
TPEPP	two-photon excited photoproduct
T term	second term in Eq. (3)
WLC	white-light continuum method for measuring δ
Γ	half-width of absorption band at half-maximum
δ	2PA cross-section
Δ	detuning factor, $E_{gi}-h\nu$
λ	wavelength
μ_{kl}	dipole moments for transitions $k \rightarrow l$
μs	microsecond, 10^{-6} s
ν	optical frequency
σ_p^+	modified Hammett substituent coefficient
Φ_F	fluorescence quantum yield
Φ_Δ	singlet oxygen quantum yield

Our work on two-photon dyes would not have been possible without the help and encouragement of several collaborators, particularly Aleksander Rebane and Mikhail Drobizhev (Montana State University, Bozeman, USA), Jean-Luc Brédas and Joseph Perry (Georgia Institute of Technology, Atlanta, USA), Karin Schmidt (Graz, Austria), and Brian Wilson (Ontario Cancer Institute, University of Toronto, Canada). We are grateful to the EPSRC, DSTL, EOARD, and DARPA for financial support. M.P. thanks the EC for an Intra-European Fellowship (MEIF-CT-2006-041629).

Received: October 27, 2008

[1] M. Göppert-Mayer, *Ann. Phys.* **1931**, *401*, 273 – 294.
[2] W. Kaiser, C. G. B. Garrett, *Phys. Rev. Lett.* **1961**, *7*, 229 – 231.
[3] W. Denk, J. H. Strickler, W. W. Webb, *Science* **1990**, *248*, 73 – 76.
[4] S. R. Marder, *Chem. Commun.* **2006**, 131 – 134.
[5] W. R. Zipfel, R. M. Williams, W. W. Webb, *Nat. Biotechnol.* **2003**, *21*, 1369 – 1377.
[6] F. Helmchen, W. Denk, *Nat. Methods* **2005**, *2*, 932 – 940.
[7] C. N. LaFratta, J. T. Fourkas, T. Baldacchini, R. A. Farrer, *Angew. Chem.* **2007**, *119*, 6352 – 6374; *Angew. Chem. Int. Ed.* **2007**, *46*, 6238 – 6258.
[8] D. A. Parthenopoulos, P. M. Rentzepis, *Science* **1989**, *245*, 843 – 845.
[9] S. Kawata, Y. Kawata, *Chem. Rev.* **2000**, *100*, 1777 – 1788.
[10] C. W. Spangler, *J. Mater. Chem.* **1999**, *9*, 2013 – 2020.
[11] T.-C. Lin, S.-J. Chung, K. S. Kim, X. Wang, G. S. He, J. Swiatkiewicz, H. E. Pudavar, P. N. Prasad, *Adv. Polym. Sci.* **2003**, *161*, 157 – 193.
[12] W. G. Fisher, W. P. Partridge, Jr., C. Dees, E. A. Wachter, *Photochem. Photobiol.* **1997**, *66*, 141 – 155.
[13] G. C. R. Ellis-Davies, *Nat. Methods* **2007**, *4*, 619 – 628.
[14] a) B. Strehmel, V. Strehmel, *Adv. Photochem.* **2007**, *29*, 111 – 354; b) M. Rumi, S. Barlow, J. Wang, J. W. Perry, S. R. Marder, *Adv. Polym. Sci.* **2008**, *213*, 1 – 95; c) G. S. He, L.-S. Tan, Q. Zheng, P. N. Prasad, *Chem. Rev.* **2008**, *108*, 1245 – 1330; d) F. Terenziani, C. Katan, E. Badaeva, S. Tretiak, M. Blanchard-Desce, *Adv. Mater.* **2008**, *20*, 4641 – 4678; e) H. M. Kim, B. R. Cho, *Chem. Commun.* **2009**, 153 – 164.
[15] Equation (2) is in SI units. The American literature mostly uses Gaussian CGS units, in which case the equivalent expression is multiplied by $16\pi^2\varepsilon_0^2$ and the electronic charge is expressed in esu. Other forms arise from various choices of the units for energy, frequency, or linewidth.
[16] P. N. Butcher, D. Cotter, *The Elements of Non-Linear Optics*, Cambridge University Press, Cambridge, **1990**.
[17] R. Loudon, *The Quantum Theory of Light*, Oxford University Press, Oxford, **1973**.
[18] R. W. Boyd, *Non-Linear Optics*, 2nd ed., Elsevier, London, **2003**.
[19] W. J. Meath, E. A. Power, *J. Phys. B* **1984**, *17*, 763 – 781.
[20] T. Kogej, D. Beljonne, F. Meyers, J. W. Perry, S. R. Marder, J. L. Brédas, *Chem. Phys. Lett.* **1998**, *298*, 1 – 6.
[21] J. R. Heflin, K. Y. Wong, O. Zamani-Khamiri, A. F. Garito, *Phys. Rev. B* **1988**, *38*, 1573 – 1576.
[22] S. N. Dixit, D. Guo, S. Mazumdar, *Phys. Rev. B* **1991**, *43*, 6781 – 6784.
[23] R. R. Birge, B. M. Pierce, *Int. J. Quantum Chem.* **1986**, *29*, 639 – 656.
[24] M. Albota, D. Beljonne, J.-L. Brédas, J. E. Ehrlich, J.-Y. Fu, A. A. Heikal, S. E. Hess, T. Kogej, M. D. Levin, S. R. Marder, D. McCord-Maughon, J. W. Perry, H. Röckel, M. Rumi, G. Subramaniam, W. W. Webb, X.-L. Wu, C. Xu, *Science* **1998**, *281*, 1653 – 1656.
[25] M. Rumi, J. E. Ehrlich, A. A. Heikal, J. W. Perry, S. Barlow, Z. Hu, D. McCord-Maughon, T. C. Parker, H. Röckel, S. Thayumanavan, S. R. Marder, D. Beljonne, J.-L. Brédas, *J. Am. Chem. Soc.* **2000**, *122*, 9500 – 9510.
[26] R. L. Martin, *J. Chem. Phys.* **2003**, *118*, 4775 – 4777.
[27] C. Katan, S. Tretiak, M. H. V. Werts, A. J. Bain, R. J. Marsh, N. Leonczek, N. Nicolaou, E. Badaeva, O. Mongin, M. Blanchard-Desce, *J. Phys. Chem. B* **2007**, *111*, 9468 – 9483.
[28] M. Drobizhev, Y. Stepanenko, A. Rebane, C. J. Wilson, T. E. O. Screen, H. L. Anderson, *J. Am. Chem. Soc.* **2006**, *128*, 12432 – 12433.
[29] M. Sheik-Bahae, A. A. Said, T.-H. Wei, D. J. Hagan, E. W. Van Stryland, *IEEE J. Quantum Electron.* **1990**, *26*, 760 – 769.
[30] K. Kamada, A. Matsunaga, K. Yoshino, *J. Opt. Soc. Am. B* **2003**, *20*, 529 – 537.
[31] C. Xu, W. W. Webb, *J. Opt. Soc. Am. B* **1996**, *13*, 481 – 491.
[32] M. Drobizhev, Y. Stepanenko, Y. Dzenis, A. Karotki, A. Rebane, P. N. Taylor, H. L. Anderson, *J. Phys. Chem. B* **2005**, *109*, 7223 – 7236.

[33] N. S. Makarov, M. Drobizhev, A. Rebane, *Opt. Express* **2008**, *16*, 4029 – 4047.

[34] Although results from *z*-scan measurements can easily be misinterpreted (R. Signorini, C. Ferrante, D. Pedron, M. Zerbetto, E. Cecchetto, M. Slaviero, I. Fortunati, E. Collini, R. Bozio, A. Abbotto, L. Beverina, G. A. Pagani, *J. Phys. Chem. A* **2008**, *112*, 4224 – 4234), thorough analysis of *z*-scan data, using a range of pulsewidths, in conjunction with pump-probe data, can give accurate 2PA cross-sections, even in spectral regions with significant 1PA and ESA; see L. A. Padilha, S. Webster, H. Hu, O. V. Przhonska, D. J. Hagan, E. W. Van Stryland, M. V. Bondar, I. G. Davydenko, Y. L. Slominsky, A. D. Kachkovski, *Chem. Phys.* **2008**, *352*, 97 – 105.

[35] W. L. Peticolas, J. P. Goldsborough, K. E. Rieckhoff, *Phys. Rev. Lett.* **1963**, *10*, 43 – 45.

[36] J. E. Ehrlich, X. L. Wu, I.-Y. S. Lee, Z.-Y. Hu, H. Röckel, S. R. Marder, J. W. Perry, *Opt. Lett.* **1997**, *22*, 1843 – 1845.

[37] B. A. Reinhardt, L. L. Brott, S. J. Clarson, A. G. Dillard, J. C. Bhatt, R. Kannan, L. Yuan, G. S. He, P. N. Prasad, *Chem. Mater.* **1998**, *10*, 1863 – 1874.

[38] G. S. He, T.-C. Lin, J. Dai, P. N. Prasad, R. Kannan, A. G. Dombroskie, R. A. Vaia, L.-S. Tan, *J. Phys. Chem.* **2004**, *120*, 5275 – 5284.

[39] L. Beverina, J. Fu, A. Leclercq, E. Zojer, P. Pacher, S. Barlow, E. W. Van Stryland, D. J. Hagan, J.-L. Brédas, S. R. Marder, *J. Am. Chem. Soc.* **2005**, *127*, 7282 – 7283.

[40] S. J. K. Pond, M. Rumi, M. D. Levin, T. C. Parker, D. Beljonne, M. W. Day, J.-L. Brédas, S. R. Marder, J. W. Perry, *J. Phys. Chem. A* **2002**, *106*, 11470 – 11480.

[41] S.-J. Chung, S. Zheng, T. Odani, L. Beverina, J. Fu, L. A. Padilha, A. Biesso, J. M. Hales, X. Zhan, K. Schmidt, A. Ye, E. Zojer, S. Barlow, D. J. Hagan, E. W. Van Stryland, Y. Yi, Z. Shuai, G. A. Pagani, J.-L. Brédas, J. W. Perry, S. R. Marder, *J. Am. Chem. Soc.* **2006**, *128*, 14444 – 14445.

[42] S.-J. Chung, K.-S. Kim, T.-C. Lin, G. S. He, J. Swiatkiewicz, P. N. Prasad, *J. Phys. Chem. B* **1999**, *103*, 10741 – 10745.

[43] R. Kannan, G. S. He, T.-C. Lin, P. N. Prasad, R. A. Vaia, L.-S. Tan, *Chem. Mater.* **2004**, *16*, 185 – 194.

[44] L. Ventelon, S. Charier, L. Moreaux, J. Mertz, M. Blanchard-Desce, *Angew. Chem.* **2001**, *113*, 2156 – 2159; *Angew. Chem. Int. Ed.* **2001**, *40*, 2098 – 2101.

[45] L. Porrès, O. Mongin, C. Katan, M. Charlot, T. Pons, J. Mertz, M. Blanchard-Desce, *Org. Lett.* **2004**, *6*, 47 – 50.

[46] C. Le Droumaguet, O. Mongin, M. H. V. Werts, M. Blanchard-Desce, *Chem. Commun.* **2005**, 2802 – 2804.

[47] O. Mongin, L. Porrès, M. Charlot, C. Katan, M. Blanchard-Desce, *Chem. Eur. J.* **2007**, *13*, 1481 – 1498.

[48] O. Varnavski, X. Yan, O. Mongin, M. Blanchard-Desce, T. Goodson III, *J. Phys. Chem. C* **2007**, *111*, 149 – 162.

[49] a) N. Isaacs, *Physical Organic Chemistry*, 2nd ed., Longman Scientific, **1995**; b) I. G. Binev, R. B. Kuzmanova, J. Kaneti, I. N. Juchnovski, *J. Chem. Soc. Perkin Trans. 2* **1982**, 1533 – 1536.

[50] Y. Tian, C.-Y. Chen, C.-C. Yang, A. C. Young, S.-H. Jang, W.-C. Chen, A. K.-Y. Jen, *Chem. Mater.* **2008**, *20*, 1977 – 1987.

[51] S. K. Lee, W. J. Yang, J. J. Choi, C. H. Kim, S.-J. Jeon, B. R. Cho, *Org. Lett.* **2005**, *7*, 323 – 326.

[52] L. Beverina, M. Crippa, P. Salice, R. Ruffo, C. Ferrante, I. Fortunati, R. Signorini, C. M. Mari, R. Bozio, A. Facchetti, G. A. Pagani, *Chem. Mater.* **2008**, *20*, 3242 – 3244.

[53] K. J. Thorley, J. M. Hales, H. L. Anderson, J. W. Perry, *Angew. Chem.* **2008**, *120*, 7203 – 7206; *Angew. Chem. Int. Ed.* **2008**, *47*, 7095 – 7098.

[54] When normalizing δ to the number of π electrons N_e, we count each double bond (C=C or C=N), triple bond (C≡C or C≡N), or donor substituent (for example, $-NMe_2$ or $-OMe$) as contributing two electrons. Thus, in porphyrinoid macrocycles, N_e is different from the electron count used to determine whether the chromophore is aromatic.

[55] M.-C. Yoon, S. B. Noh, A. Tsuda, Y. Nakamura, A. Osuka, D. Kim, *J. Am. Chem. Soc.* **2007**, *129*, 10080 – 10081.

[56] T. K. Ahn, K. S. Kim, D. Y. Kim, S. B. Noh, N. Aratani, C. Ikeda, A. Osuka, D. Kim, *J. Am. Chem. Soc.* **2006**, *128*, 1700 – 1704.

[57] Y. Nakamura, S. Y. Jang, T. Tanaka, N. Aratani, J. M. Lim, K. S. Kim, D. Kim, A. Osuka, *Chem. Eur. J.* **2008**, *14*, 8279 – 8289.

[58] S. Easwaramoorthi, S. Y. Jang, Z. S. Yoon, J. M. Lim, C.-W. Lee, C.-L. Mai, Y.-C. Liu, C.-Y. Yeh, J. Vura-Weis, M. R. Wasielewski, D. Kim, *J. Phys. Chem. A* **2008**, *112*, 6563 – 6570.

[59] J. O. Morley, *Int. J. Quantum Chem.* **1993**, *46*, 19 – 26.

[60] V. S. Lin, S. G. DiMagno, M. J. Therien, *Science* **1994**, *264*, 1105 – 1111.

[61] H. L. Anderson, *Inorg. Chem.* **1994**, *33*, 972 – 981.

[62] M. Drobizhev, F. Meng, A. Rebane, Y. Stepanenko, E. Nickel, C. W. Spangler, *J. Phys. Chem. B* **2006**, *110*, 9802 – 9814.

[63] M. Drobizhev, Y. Stepanenko, Y. Dzenis, A. Karotki, A. Rebane, P. N. Taylor, H. L. Anderson, *J. Am. Chem. Soc.* **2004**, *126*, 15352 – 15353.

[64] M. J. Frampton, H. Akdas, A. R. Cowley, J. E. Rogers, J. E. Slagle, P. A. Fleitz, M. Drobizhev, A. Rebane, H. L. Anderson, *Org. Lett.* **2005**, *7*, 5365 – 5368.

[65] H. A. Collins, M. Khurana, E. H. Moriyama, A. Mariampillai, E. Dahlstedt, M. Balaz, M. K. Kuimova, M. Drobizhev, V. X. D. Yang, D. Phillips, A. Rebane, B. C. Wilson, H. L. Anderson, *Nat. Photonics* **2008**, *2*, 420 – 424.

[66] M. O. Senge, M. Fazekas, E. G. A. Notaras, W. J. Blau, M. Zawadzka, O. B. Locos, E. M. Ni Mhuircheartaigh, *Adv. Mater.* **2007**, *19*, 2737 – 2774.

[67] J. Arnbjerg, A. Jiménez-Banzo, M. J. Paterson, S. Nonell, J. I. Borrell, O. Christiansen, P. R. Ogilby, *J. Am. Chem. Soc.* **2007**, *129*, 5188 – 5199.

[68] K. S. Kim, J. M. Lim, A. Osuka, D. Kim, *J. Photochem. Photobiol. C* **2008**, *9*, 13 – 28.

[69] K. Kurotobi, K. S. Kim, S. B. Noh, D. Kim, A. Osuka, *Angew. Chem.* **2006**, *118*, 4048 – 4051; *Angew. Chem. Int. Ed.* **2006**, *45*, 3944 – 3947.

[70] T. K. Ahn, J. H. Kwon, D. Y. Kim, D. W. Cho, D. H. Jeong, S. K. Kim, M. Suzuki, S. Shimizu, A. Osuka, D. Kim, *J. Am. Chem. Soc.* **2005**, *127*, 12856 – 12861.

[71] a) Y. Tanaka, S. Saito, S. Mori, N. Aratani, H. Shinokubo, N. Shibata, Y. Higuchi, Z. S. Yoon, K. S. Kim, S. B. Noh, J. K. Park, D. Kim, A. Osuka, *Angew. Chem.* **2008**, *120*, 693 – 696; *Angew. Chem. Int. Ed.* **2008**, *47*, 681 – 684; b) J. M. Lim, Z. S. Yoon, J.-Y. Shin, K. S. Kim, M.-C. Yoon, D. Kim, *Chem. Commun.* **2009**, 261 – 273.

[72] H. Rath, J. Sankar, V. PrabhuRaja, T. K. Chandrashekar, A. Nag, D. Goswami, *J. Am. Chem. Soc.* **2005**, *127*, 11608 – 11609.

[73] M. Williams-Harry, A. Bhaskar, G. Ramakrishna, T. Goodson, III, M. Imamura, A. Mawatari, K. Nakao, H. Enozawa, T. Nishinaga, M. Iyoda, *J. Am. Chem. Soc.* **2008**, *130*, 3252 – 3253.

[74] Y.-Z. Cui, Q. Fang, G. Xue, G.-B. Xu, L. Yin, W.-T. Yu, *Chem. Lett.* **2005**, *34*, 644 – 645.

[75] A. Bhaskar, R. Guda, M. M. Haley, T. Goodson III, *J. Am. Chem. Soc.* **2006**, *128*, 13972 – 13973.

[76] M. Drobizhev, A. Karotki, A. Rebane, C. W. Spangler, *Opt. Lett.* **2001**, *26*, 1081 – 1083.

[77] a) M. K. Kuimova, M. Hoffmann, M. U. Winters, M. Eng, M. Balaz, I. P. Clark, H. A. Collins, S. M. Tavender, C. J. Wilson, B. Albinsson, H. L. Anderson, A. W. Parker, D. Phillips, *Photochem. Photobiol. Sci.* **2007**, *6*, 675 – 682; b) M. J. Frampton, G. Accorsi, N. Armaroli, J. E. Rogers, P. A. Fleitz, K. J. McEwan, H. L. Anderson, *Org. Biomol. Chem.* **2007**, *5*, 1056 – 1061.

[78] S. M. Kuebler, M. Rumi in *Encyclopedia of Modern Optics*, *Vol. III*, Elsevier, Oxford, **2005**, pp. 189 – 206.

[79] X. Wang, L. J. Krebs, M. Al-Nuri, H. E. Pudavar, S. Ghosal, C. Liebow, A. A. Nagy, A. V. Schally, P. N. Prasad, *Proc. Natl. Acad. Sci. USA* **1999**, *96*, 11081 – 11084.
[80] a) H. M. Kim, B. H. Jeong, J.-Y. Hyon, M. J. An, M. S. Seo, J. H. Hong, K. J. Lee, C. H. Kim, T. Joo, S.-C. Hong, B. R. Cho, *J. Am. Chem. Soc.* **2008**, *130*, 4246 – 4247; b) H. M. Kim, M. J. An, J. H. Hong, B. H. Jeong, O. Kwon, J.-Y. Hyon, S.-C. Hong, K. J. Lee, B. R. Cho, *Angew. Chem.* **2008**, *120*, 2263 – 2266; *Angew. Chem. Int. Ed.* **2008**, *47*, 2231 – 2234.
[81] S. J. K. Pond, O. Tsutsumi, M. Rumi, O. Kwon, E. Zojer, J.-L. Brédas, S. R. Marder, J. W. Perry, *J. Am. Chem. Soc.* **2004**, *126*, 9291 – 9306.
[82] H. M. Kim, M.-Y. Jeong, H. C. Ahn, S.-J. Jeon, B. R. Cho, *J. Org. Chem.* **2004**, *69*, 5749 – 5751.
[83] H. C. Ahn, S. K. Yang, H. M. Kim, S. Li, S.-J. Jeon, B. R. Cho, *Chem. Phys. Lett.* **2005**, *410*, 312 – 315.
[84] R. Bozio, E. Cecchetto, G. Fabbrini, C. Ferrante, M. Maggini, E. Menna, D. Pedron, R. Riccò, R. Signorini, M. Zerbetto, *J. Phys. Chem. A* **2006**, *110*, 6459 – 6464.
[85] S. Sumalekshmy, M. M. Henary, N. Siegel, P. V. Lawson, Y. Wu, K. Schmidt, J.-L. Brédas, J. W. Perry, C. J. Fahrni, *J. Am. Chem. Soc.* **2007**, *129*, 11888 – 11889.
[86] A. Bhaskar, G. Ramakrishna, R. J. Twieg, T. Goodson III, *J. Phys. Chem. C* **2007**, *111*, 14607 – 14611.
[87] H. M. Kim, M. S. Seo, M. J. An, J. H. Hong, Y. S. Tian, J. H. Choi, O. Kwon, K. J. Lee, B. R. Cho, *Angew. Chem.* **2008**, *120*, 5245 – 5248; *Angew. Chem. Int. Ed.* **2008**, *47*, 5167 – 5170.
[88] C. Huang, J. Fan, X. Peng, Z. Lin, B. Guo, A. Ren, J. Cui, S. Sun, *J. Photochem. Photobiol. A* **2008**, *199*, 144 – 149.
[89] M.-H. Ha-Thi, M. Penhoat, D. Drouin, M. Blanchard-Desce, V. Michelet, I. Leray, *Chem. Eur. J.* **2008**, *14*, 5941 – 5950.
[90] Z.-Q. Liu, M. Shi, F.-Y. Li, Q. Fang, Z.-H. Chen, T. Yi, C.-H. Huang, *Org. Lett.* **2005**, *7*, 5481 – 5484.
[91] S. Charier, O. Ruel, J.-B. Baudin, D. Alcor, J.-F. Allemand, A. Meglio, L. Jullien, *Angew. Chem.* **2004**, *116*, 4889 – 4892; *Angew. Chem. Int. Ed.* **2004**, *43*, 4785 – 4788.
[92] M. Matsuzaki, G. C. R. Ellis-Davies, T. Nemoto, Y. Miyashita, M. Iino, H. Kasai, *Nat. Neurosci.* **2001**, *4*, 1086 – 1092.
[93] C. D. Harvey, K. Svoboda, *Nature* **2007**, *450*, 1195 – 1200.
[94] T. Furuta, S. S.-H. Wang, J. L. Dantzker, T. M. Dore, W. J. Bybee, E. M. Callaway, W. Denk, R. Y. Tsien, *Proc. Natl. Acad. Sci. USA* **1999**, *96*, 1193 – 1200.
[95] S. Gug, S. Charon, A. Specht, K. Alarcon, D. Ogden, B. Zietz, J. Léonard, S. Haacke, F. Bolze, J.-F. Nicoud, M. Goeldner, *ChemBioChem* **2008**, *9*, 1303 – 1307.
[96] A. Momotake, N. Lindegger, E. Niggli, R. J. Barsotti, G. C. R. Ellis-Davies, *Nat. Methods* **2006**, *3*, 35 – 40.
[97] S. Wecksler, A. Mikhailovsky, P. C. Ford, *J. Am. Chem. Soc.* **2004**, *126*, 13566 – 13567.
[98] A. P. Goodwin, J. L. Mynar, Y. Ma, G. R. Fleming, J. M. J. Fréchet, *J. Am. Chem. Soc.* **2005**, *127*, 9952 – 9953.
[99] S. B. Brown, E. A. Brown, I. Walker, *Lancet Oncol.* **2004**, *5*, 497 – 508.
[100] R. Marchesini, E. Melloni, G. Pezzoni, G. Savi, F. Zunino, F. Docchio, G. Fava, *Lasers Surg. Med.* **1986**, *6*, 323 – 327.
[101] P. Lenz, *Photochem. Photobiol.* **1995**, *62*, 333 – 338.
[102] J. D. Bhawalkar, N. D. Kumar, C.-F. Zhao, P. N. Prasad, *J. Clin. Laser Med. Surg.* **1997**, *15*, 201 – 204.
[103] M. Khurana, H. A. Collins, A. Karotki, H. L. Anderson, D. T. Cramb, B. C. Wilson, *Photochem. Photobiol.* **2007**, *83*, 1441 – 1448.
[104] K. S. Samkoe, A. A. Clancy, A. Karotki, B. C. Wilson, D. T. Cramb, *J. Biol. Opt.* **2007**, *12*, 034025/034021 – 034025/034014.
[105] M. A. Oar, W. R. Dichtel, J. M. Serin, J. M. J. Fréchet, J. E. Rogers, J. E. Slagle, P. A. Fleitz, L.-S. Tan, T. Y. Ohulchanskyy, P. N. Prasad, *Chem. Mater.* **2006**, *18*, 3682 – 3692.
[106] a) C. W. Spangler, J. R. Starkley, A. Rebane, F. Meng, A. Gong, M. Drobizhev, *Proc. SPIE* **2006**, *6139*, 61390X; b) J. R. Starkey, A. K. Rebane, M. A. Drobizhev, F. Meng, A. Gong, A. Elliott, K. McInnerney, C. W. Spangler, *Clin. Cancer Res.* **2008**, *14*, 6564 – 6573.
[107] S. Kim, T. Y. Ohulchanskyy, H. E. Pudavar, R. K. Pandey, P. N. Prasad, *J. Am. Chem. Soc.* **2007**, *129*, 2669 – 2675.
[108] L. Beverina, M. Crippa, M. Landenna, R. Ruffo, P. Salice, F. Silvestri, S. Versari, A. Villa, L. Ciaffoni, E. Collini, C. Ferrante, S. Bradamante, C. M. Mari, R. Bozio, G. A. Pagani, *J. Am. Chem. Soc.* **2008**, *130*, 1894 – 1902.
[109] K. Ogawa, H. Hasegawa, Y. Inaba, Y. Kobuke, H. Inouye, Y. Kanemitsu, E. Kohno, T. Hirano, S.-i. Ogura, I. Okura, *J. Med. Chem.* **2006**, *49*, 2276 – 2283.
[110] B. Jia, J. Li, M. Gu, *Aust. J. Chem.* **2007**, *60*, 484 – 495.
[111] K.-S. Lee, D.-Y. Yang, S. H. Park, R. H. Kim, *Polym. Adv. Technol.* **2006**, *17*, 72 – 82.
[112] S. H. Wong, M. Thiel, P. Brodersen, D. Fenske, G. A. Ozin, M. Wegener, G. von Freymann, *Chem. Mater.* **2007**, *19*, 4213 – 4221.
[113] S. M. Kuebler, K. L. Braun, W. Zhou, J. K. Cammack, T. Yu, C. K. Ober, S. R. Marder, J. W. Perry, *J. Photochem. Photobiol. A* **2003**, *158*, 163 – 170.
[114] J. Scrimgeour, D.Phil. Thesis, Department of Physics, University of Oxford, Oxford, UK, **2005**.
[115] J. Scrimgeour, D. N. Sharp, C. F. Blanford, O. M. Roche, R. G. Denning, A. J. Turberfield, *Adv. Mater.* **2006**, *18*, 1557 – 1560.
[116] N. Tétreault, G. von Freymann, M. Deubel, M. Hermatschweiler, F. Pérez-Willard, S. John, M. Wegener, G. A. Ozin, *Adv. Mater.* **2006**, *18*, 457 – 460.
[117] W. Haske, V. W. Chen, J. M. Hales, W. Dong, S. Barlow, S. R. Marder, J. W. Perry, *Opt. Express* **2007**, *15*, 3426 – 3436.
[118] E. Walker, P. M. Rentzepis, *Nat. Photonics* **2008**, *2*, 406 – 408.
[119] J. T. Dy, R. Maeda, Y. Nagatsuka, K. Ogawa, K. Kamada, K. Ohta, Y. Kobuke, *Chem. Commun.* **2007**, 5170 – 5172.
[120] H. Tian, Y. Feng, *J. Mater. Chem.* **2008**, *18*, 1617 – 1622.
[121] M. P. Joshi, J. Swiatkiewicz, F. Xu, P. N. Prasad, *Opt. Lett.* **1998**, *23*, 1742 – 1744.
[122] J. Träger, H.-C. Kim, N. Hampp, *Nat. Photonics* **2007**, *1*, 509 – 511.
[123] B. N. G. Giepmans, S. R. Adams, M. H. Ellisman, R. Y. Tsien, *Science* **2006**, *312*, 217 – 224.
[124] M. Drobizhev, N. S. Makarov, T. Hughes, A. Rebane, *J. Phys. Chem. B* **2007**, *111*, 14051 – 14054.

